Algorithm 961: Fortran 77 Subroutines for the Solution of Skew-Hamiltonian/Hamiltonian Eigenproblems

PETER BENNER, Max Planck Institute for Dynamics of Complex Technical Systems, Magdeburg
VASILE SIMA, National Institute for Research and Development in Informatics, Bucharest
MATTHIAS VOIGT, Institut für Mathematik, Technische Universität Berlin, Berlin

Skew-Hamiltonian/Hamiltonian matrix pencils $\lambda\mathcal{S} - \mathcal{H}$ appear in many applications, including linear-quadratic optimal control problems, $\mathcal{H}_\infty$-optimization, certain multibody systems, and many other areas in applied mathematics, physics, and chemistry. In these applications it is necessary to compute certain eigenvalues and/or corresponding deflating subspaces of these matrix pencils. Recently developed methods exploit and preserve the skew-Hamiltonian/Hamiltonian structure and hence increase the reliability, accuracy, and performance of the computations. In this article, we describe the corresponding algorithms which have been implemented in the style of subroutines of the Subroutine Library in Control Theory (SLICOT). Furthermore, we address some of their applications. We describe variants for real and complex problems, as well as implementation details and perform numerical tests using real-world examples to demonstrate the superiority of the new algorithms compared to standard methods.

Categories and Subject Descriptors: D.3.2 [**Programming Languages**]: Language Classifications—*Fortran 77*; G.1.3 [**Numerical Analysis**]: Numerical Linear Algebra—*Eigenvalues and eigenvectors (direct and iterative methods)*

General Terms: Algorithms, Documentation, Reliability

Additional Key Words and Phrases: Deflating subspaces, eigenvalue reordering, generalized eigenvalues, generalized schur form, skew-Hamiltonian/Hamiltonian matrix pencil, software, structure-preservation

ACM Reference Format:
Peter Benner, Vasile Sima, and Matthias Voigt. 2016. Algorithm 961: Fortran 77 subroutines for the solution of skew-Hamiltonian/Hamiltonian eigenproblems. ACM Trans. Math. Softw. 42, 3, Article 24 (May 2016), 26 pages.
DOI: http://dx.doi.org/10.1145/2818313

1. INTRODUCTION

In this article, we discuss algorithms for the solution of generalized eigenvalue problems with skew-Hamiltonian/Hamiltonian structure. We are interested in the computation of certain eigenvalues and corresponding deflating subspaces. In this work, we deal with the following algebraic structures [Benner et al. 2002]. As a notational convention, we use calligraphic letters for block matrices and standard letters for ordinary matrices. Moreover, we denote by $\mathbb{R}[\lambda]^{n\times n}$ and $\mathbb{C}[\lambda]^{n\times n}$ the rings of polynomials with coefficients in $\mathbb{R}^{n\times n}$ and $\mathbb{C}^{n\times n}$, respectively.

Definition 1.1. Let $\mathcal{J} := \left[\begin{smallmatrix} 0 & I_n \\ -I_n & 0 \end{smallmatrix}\right]$, where I_n is the $n \times n$ identity matrix. For brevity of notation, we do not indicate the dimension of the matrix $\mathcal{J}$ and use it for all possible values of n.

(i) A matrix $\mathcal{H} \in \mathbb{C}^{2n\times 2n}$ is *Hamiltonian* if $(\mathcal{H}\mathcal{J})^H = \mathcal{H}\mathcal{J}$.
(ii) A matrix $\mathcal{S} \in \mathbb{C}^{2n\times 2n}$ is *skew-Hamiltonian* if $(\mathcal{S}\mathcal{J})^H = -\mathcal{S}\mathcal{J}$.
(iii) A matrix pencil $\lambda\mathcal{S} - \mathcal{H} \in \mathbb{C}[\lambda]^{2n\times 2n}$ is *skew-Hamiltonian/Hamiltonian* if $\mathcal{S}$ is skew-Hamiltonian and $\mathcal{H}$ is Hamiltonian.
(iv) A matrix $\mathcal{S} \in \mathbb{C}^{2n\times 2n}$ is *symplectic* if $\mathcal{S}\mathcal{J}\mathcal{S}^H = \mathcal{J}$.
(v) A matrix $\mathcal{U} \in \mathbb{C}^{2n\times 2n}$ is *unitary symplectic* if $\mathcal{U}\mathcal{J}\mathcal{U}^H = \mathcal{J}$ and $\mathcal{U}\mathcal{U}^H = I_{2n}$.

Note that a similar definition can be given for real matrices. As a convention, all following considerations also hold for real skew-Hamiltonian/Hamiltonian matrix pencils. Then, all matrices $\cdot^H$ must be replaced by $\cdot^T$, all (skew-)Hermitian matrices become (skew-)symmetric, and unitary matrices become orthogonal. More significant differences to the complex case are explicitly mentioned.

Skew-Hamiltonian/Hamiltonian matrix pencils satisfy certain properties, which we will review briefly. Every skew-Hamiltonian/Hamiltonian matrix pencil can be written as

$$\lambda\mathcal{S} - \mathcal{H} = \lambda\begin{bmatrix} A & D \\ E & A^H \end{bmatrix} - \begin{bmatrix} B & F \\ G & -B^H \end{bmatrix}$$

with skew-Hermitian matrices D, E and Hermitian matrices F, G. If λ_0 is a (generalized) eigenvalue of $\lambda\mathcal{S} - \mathcal{H}$, so is also $-\overline{\lambda}_0$. In other words, eigenvalues which are not purely imaginary, occur in pairs. For real skew-Hamiltonian/Hamiltonian matrix pencils, we also have a pairing of complex conjugate eigenvalues (i.e., if λ_0 is an eigenvalue of $\lambda\mathcal{S} - \mathcal{H}$, so are also $\overline{\lambda}_0$, $-\lambda_0$, $-\overline{\lambda}_0$). This leads to eigenvalue pairs $(\lambda_0, -\lambda_0)$ if λ is purely real or purely imaginary, or otherwise to eigenvalue quadruples $(\lambda_0, \overline{\lambda}_0, -\lambda_0, -\overline{\lambda}_0)$.

The structure of skew-Hamiltonian/Hamiltonian matrix pencils is preserved under *$\mathcal{J}$-congruence transformations*; that is, $\lambda\widetilde{\mathcal{S}} - \widetilde{\mathcal{H}} := \mathcal{J}\mathcal{P}^H\mathcal{J}^T(\lambda\mathcal{S} - \mathcal{H})\mathcal{P}$ with nonsingular $\mathcal{P}$ is again skew-Hamiltonian/Hamiltonian. If we choose $\mathcal{P}$ unitary, we additionally preserve the condition of the problem. In this way, there is hope that we can choose a unitary $\mathcal{J}$-congruence transformation to transform $\lambda\mathcal{S} - \mathcal{H}$ into a condensed form which reveals its eigenvalues and deflating subspaces. A suitable candidate for this condensed form is the *structured Schur form*; that is, we compute a unitary matrix $\mathcal{Q}$ such that

$$\mathcal{J}\mathcal{Q}^H\mathcal{J}^T(\lambda\mathcal{S} - \mathcal{H})\mathcal{Q} = \lambda\begin{bmatrix} S_{11} & S_{12} \\ 0 & S_{11}^H \end{bmatrix} - \begin{bmatrix} H_{11} & H_{12} \\ 0 & -H_{11}^H \end{bmatrix}$$

with the subpencil $\lambda S_{11} - H_{11}$ in generalized Schur form, where S_{11} is upper triangular, H_{11} is upper triangular (upper quasi-triangular in the real case), S_{12} is skew-Hermitian, and H_{12} is Hermitian. However, such a structured Schur form does *not* necessarily exist. Conditions for the existence are proven in Mehl [1999, 2000] for the complex case or in Voigt [2010] for the real case. This problem can be circumvented by embedding $\lambda\mathcal{S} - \mathcal{H}$ into a skew-Hamiltonian/Hamiltonian matrix pencil of double dimension in an appropriate way, as explained in Section 3.

Skew-Hamiltonian/Hamiltonian pencils are closely related to *even pencils* $\lambda\mathcal{E} - \mathcal{A}$; that is, $\mathcal{E} = -\mathcal{E}^H$ and $\mathcal{A} = \mathcal{A}^H$. It is easy to see that if $\lambda\mathcal{S} - \mathcal{H}$ is skew-Hamiltonian/Hamiltonian, then $\mathcal{J}(\lambda\mathcal{S} - \mathcal{H})$ is even. However, the converse is not true. If $\lambda\mathcal{E} - \mathcal{A} \in \mathbb{C}[\lambda]^{k\times k}$ is even and of odd dimension, then it cannot be transformed directly to skew-Hamiltonian/Hamiltonian structure. Instead, one has to inflate the pencil and introduce one artificial infinite eigenvalue. Define the number $r := k \bmod 2$. Then, the pencil

$$\lambda\mathcal{S} - \mathcal{H} := \mathcal{J}\left(\begin{bmatrix} \lambda\mathcal{E} - \mathcal{A} & 0 \\ 0 & I_r \end{bmatrix}\right)$$

is skew-Hamiltonian/Hamiltonian.

Usually, the eigenvalue problems that are obtained in practice are even. In this case, we have to do the preceding transformation to skew-Hamiltonian/Hamiltonian form. Moreover, sometimes the pencils are singular or have a higher index. Then it is often necessary to remove the singular and higher-index parts first, so that one works with a well-behaved eigenvalue problem [Byers et al. 2007; Brüll and Mehrmann 2007].

Throughout this article, we denote by $\Lambda_-(\mathcal{S},\mathcal{H})$, $\Lambda_0(\mathcal{S},\mathcal{H})$, $\Lambda_+(\mathcal{S},\mathcal{H})$ the set of finite eigenvalues of $\lambda\mathcal{S} - \mathcal{H}$ with negative, zero, and positive real parts, respectively. The set of all eigenvalues is denoted by $\Lambda(\mathcal{S},\mathcal{H})$. Similarly, we denote by $\mathrm{Defl}_-(\mathcal{S},\mathcal{H})$, $\mathrm{Defl}_0(\mathcal{S},\mathcal{H})$, $\mathrm{Defl}_+(\mathcal{S},\mathcal{H})$, and $\mathrm{Defl}_\infty(\mathcal{S},\mathcal{H})$ the right deflating subspaces corresponding to $\Lambda_-(\mathcal{S},\mathcal{H})$, $\Lambda_0(\mathcal{S},\mathcal{H})$, $\Lambda_+(\mathcal{S},\mathcal{H})$, and the infinite eigenvalues, respectively.

2. APPLICATIONS

2.1. Linear-Quadratic Optimal Control

First, we consider the continuous-time, infinite horizon, linear-quadratic optimal control problem:
Choose a control function $u : [0,\infty) \to \mathbb{R}^m$ to minimize the cost functional

$$\mathcal{J}(x,u) := \int_0^\infty \begin{bmatrix} x(t) \\ u(t) \end{bmatrix}^T \begin{bmatrix} Q & S \\ S^T & R \end{bmatrix} \begin{bmatrix} x(t) \\ u(t) \end{bmatrix} \mathrm{d}t \tag{1}$$

subject to the linear time-invariant *descriptor system*

$$E\dot{x}(t) = Ax(t) + Bu(t), \quad Ex(0) = Ex_0. \tag{2}$$

Here, $u : [0,\infty) \to \mathbb{R}^m$ is a control input, $x : [0,\infty) \to \mathbb{R}^n$ is the state, and $\lambda E - A \in \mathbb{R}[\lambda]^{n\times n}$ is regular, $B \in \mathbb{R}^{n\times m}$, $Q = Q^T \in \mathbb{R}^{n\times n}$, $R = R^T \in \mathbb{R}^{m\times m}$, $S \in \mathbb{R}^{n\times m}$. For well-posedness, the matrix R is assumed to be positive semidefinite.

Typically, in addition to minimizing Equation (1), the control $u(\cdot)$ must make $x(\cdot)$ asymptotically stable. Under some regularity conditions, the application of the maximum principle [Pontryagin et al. 1962; Mehrmann 1991] yields as a necessary optimality condition that the control $u(\cdot)$ satisfies the two-point boundary value problem of Euler-Lagrange equations

$$\mathcal{E}\begin{bmatrix} \dot{\mu}(t) \\ \dot{x}(t) \\ \dot{u}(t) \end{bmatrix} = \mathcal{A}\begin{bmatrix} \mu(t) \\ x(t) \\ u(t) \end{bmatrix}, \quad Ex(0) = Ex_0, \quad \lim_{t\to\infty} E^T\mu(t) = 0$$

with the even matrix pencil

$$\lambda\mathcal{E} - \mathcal{A} = \lambda\begin{bmatrix} 0 & E & 0 \\ -E^T & 0 & 0 \\ 0 & 0 & 0 \end{bmatrix} - \begin{bmatrix} 0 & A & B \\ A^T & Q & S \\ B^T & S^T & R \end{bmatrix}. \tag{3}$$

Under certain stabilizability conditions, the optimal control $u_*(\cdot)$ that stabilizes the descriptor system in Equation (2) can be constructed via a stabilizing solution of certain matrix equations. For the case that R is positive definite, this includes several versions of generalized algebraic Riccati equations [Mehrmann 1991; Kawamoto et al. 1999], for the general case with possibly singular R, one has to turn to so-called (descriptor) Lur'e equations [Reis 2011; Reis et al. 2015; Voigt 2015]. In all cases, the desired solution can be determined using the deflating subspaces of $\lambda\mathcal{E} - \mathcal{A}$ to the eigenvalues with negative real parts and to some purely imaginary and infinite eigenvalues.

2.2. $\mathcal{H}_\infty$-Optimization

Similar structures as in Subsection 2.1 occur in $\mathcal{H}_\infty$-optimization [Losse et al. 2008]. Consider a descriptor system of the form

$$\mathbf{P}: \quad \begin{cases} E\dot{x}(t) = Ax(t) + B_1w(t) + B_2u(t), \\ \;\; z(t) = C_1x(t) + D_{11}w(t) + D_{12}u(t), \\ \;\; y(t) = C_2x(t) + D_{21}w(t) + D_{22}u(t), \end{cases} \tag{4}$$

where $\lambda E - A \in \mathbb{R}[\lambda]^{n\times n}$ is regular, $B_i \in \mathbb{R}^{n\times m_i}$, $C_i \in \mathbb{R}^{p_i\times n}$, and $D_{ij} \in \mathbb{R}^{p_i\times m_j}$ for $i, j = 1, 2$. In this system, $x : [0,\infty) \to \mathbb{R}^n$ is the state, $u : [0,\infty) \to \mathbb{R}^{m_2}$ is the control input, and $w : [0,\infty) \to \mathbb{R}^{m_1}$ is an exogenous input that may include noise, linearization errors, and unmodeled dynamics. The function $y : [0,\infty) \to \mathbb{R}^{p_2}$ contains measured outputs, whereas $z : [0,\infty) \to \mathbb{R}^{p_1}$ is a regulated output or an estimation error.

The $\mathcal{H}_\infty$ control problem is naturally formulated in the frequency domain. For this we need the space $\mathcal{RH}_\infty^{p\times m}$ which consists of all real-rational $\mathbb{C}^{p\times m}$-valued functions that are analytic and bounded in the open right half-plane $\mathbb{C}^+$. For $G \in \mathcal{RH}_\infty^{p\times m}$, the $\mathcal{H}_\infty$-norm is defined by

$$\|G\|_{\mathcal{H}_\infty} := \sup_{s\in\mathbb{C}^+} \sigma_{\max}(G(s)) = \sup_{\omega\in\mathbb{R}} \sigma_{\max}(G(\mathrm{i}\omega)),$$

where $\sigma_{\max}(M)$ denotes the largest singular value of the matrix M. In robust control, $\|G\|_{\mathcal{H}_\infty}$ is used as a measure of the worst-case influence of the disturbances w on the output z, where, in this case, G is the transfer function mapping noise or disturbance inputs to error signals [Zhou and Doyle 1998]. Solving the optimal $\mathcal{H}_\infty$ control problem is the task of designing a dynamic controller

$$\mathbf{K}: \quad \begin{cases} \widehat{E}\dot{\widehat{x}}(t) = \widehat{A}\widehat{x}(t) + \widehat{B}y(t), \\ \;\; u(t) = \widehat{C}\widehat{x}(t) + \widehat{D}y(t), \end{cases} \tag{5}$$

with regular $\lambda\widehat{E} - \widehat{A} \in \mathbb{R}[\lambda]^{N\times N}$, $\widehat{B} \in \mathbb{R}^{N\times p_2}$, $\widehat{C} \in \mathbb{R}^{m_2\times N}$, $\widehat{D} \in \mathbb{R}^{m_2\times p_2}$ such that the closed-loop system resulting from inserting Equation (5) into Equation (4), that is,

$$\begin{aligned} E\dot{x}(t) &= (A + B_2\widehat{D}Z_1C_2)x(t) + B_2Z_2\widehat{C}\widehat{x}(t) + (B_1 + B_2\widehat{D}Z_1D_{21})w(t), \\ \widehat{E}\dot{\widehat{x}}(t) &= \widehat{B}Z_1C_2x(t) + (\widehat{A} + \widehat{B}Z_1D_{22}\widehat{C})\widehat{x}(t) + \widehat{B}Z_1D_{21}w(t), \\ z(t) &= (C_1 + D_{12}Z_2\widehat{D}C_2)x(t) + D_{12}Z_2\widehat{C}\widehat{x}(t) + (D_{11} + D_{12}\widehat{D}Z_1D_{21})w(t), \end{aligned} \tag{6}$$

with $Z_1 = (I_{p_2} - D_{22}\widehat{D})^{-1}$, and $Z_2 = (I_{m_2} - \widehat{D}D_{22})^{-1}$ has the following properties:

(i) System (6) is internally stable; that is, the solution $\left[\begin{smallmatrix} x(t) \\ \widehat{x}(t) \end{smallmatrix}\right]$ of the system with $w \equiv 0$ is asymptotically stable, i.e., $\lim_{t\to\infty}\left[\begin{smallmatrix} x(t) \\ \widehat{x}(t) \end{smallmatrix}\right] = 0$.

(ii) The closed-loop transfer function T_{zw} from w to z satisfies $T_{zw} \in \mathcal{RH}_\infty^{p_1\times m_1}$ and is minimized in the $\mathcal{H}_\infty$-norm.

Closely related to the optimal $\mathcal{H}_\infty$ control problem is the modified optimal $\mathcal{H}_\infty$ control problem. For a given descriptor system of the form in Equation (4), we search the infimum value γ for which there exists an internally stabilizing dynamic controller of the form in Equation (5) such that the corresponding closed-loop system in Equation (6) satisfies $T_{zw} \in \mathcal{RH}_\infty^{p_1\times m_1}$ with $\|T_{zw}\|_{\mathcal{H}_\infty} < \gamma$. For the construction of optimal controllers, one can make use of the following *even* matrix pencils (see Poppe et al. [2009] for a definition and related software)

$$\lambda \mathcal{E}_H - \mathcal{A}_H(\gamma) = \left[\begin{array}{cc|ccc} 0 & -\lambda E^T - A^T & 0 & 0 & -C_1^T \\ \lambda E - A & 0 & -B_1 & -B_2 & 0 \\ \hline 0 & -B_1^T & -\gamma^2 I_{m_1} & 0 & -D_{11}^T \\ 0 & -B_2^T & 0 & 0 & -D_{12}^T \\ -C_1 & 0 & -D_{11} & -D_{12} & -I_{p_1} \end{array}\right], \tag{7}$$

and

$$\lambda \mathcal{E}_J - \mathcal{A}_J(\gamma) = \left[\begin{array}{cc|ccc} 0 & -\lambda E - A & 0 & 0 & -B_1 \\ \lambda E^T - A^T & 0 & -C_1^T & -C_2^T & 0 \\ \hline 0 & -C_1 & -\gamma^2 I_{p_1} & 0 & -D_{11} \\ 0 & -C_2 & 0 & 0 & -D_{12} \\ -B_1^T & 0 & -D_{11}^T & -D_{12}^T & -I_{m_1} \end{array}\right]. \tag{8}$$

Using appropriate deflating subspaces of the matrix pencils in Equations (7) and (8), it is possible to state conditions for the existence of an optimal $\mathcal{H}_\infty$ controller. Then we can check if these conditions are fulfilled for a given value of γ. Using a bisection scheme, we can iteratively refine γ until a desired accuracy is achieved (see Losse et al. [2008] and Benner et al. [2008b] for details). Finally, when a suboptimal value γ has been found, one can compute the actual controller. The controller formulas are rather cumbersome and, therefore, they are omitted. For details, see Losse [2012].

2.3. $\mathcal{H}_\infty$-Norm Computation

Finally, we briefly describe a method to compute the $\mathcal{H}_\infty$-norm of an LTI system using even matrix pencils [Benner et al. 2012a, 2012b]. This norm plays an important role in robust control or model order reduction (see Antoulas [2005], Mehrmann and Stykel [2005], and Zhou and Doyle [1998] and references therein). Consider a descriptor system

$$\begin{aligned} E\dot{x}(t) &= Ax(t) + Bu(t), \\ y(t) &= Cx(t) + Du(t), \end{aligned} \tag{9}$$

with regular $\lambda E - A \in \mathbb{R}[\lambda]^{n\times n}$, $B \in \mathbb{R}^{n\times m}$, $C \in \mathbb{R}^{p\times n}$, $D \in \mathbb{R}^{p\times m}$, and state $x : [0,\infty) \to \mathbb{R}^n$, control input $u : [0,\infty) \to \mathbb{R}^m$, and output $y : [0,\infty) \to \mathbb{R}^p$. For such a system, the transfer function is given by

$$G(s) := C\,(sE - A)^{-1}\,B + D,$$

which directly maps inputs to outputs in the frequency domain [Dai 1989]. Assume that $G \in \mathcal{RH}_\infty^{p\times m}$ and consider the even matrix pencils

$$\lambda \mathcal{E} - \mathcal{A}(\gamma) := \left[\begin{array}{cc|cc} 0 & \lambda E - A & 0 & -B \\ -\lambda E^T - A^T & 0 & -C^T & 0 \\ \hline 0 & -C & -\gamma I_p & D \\ -B^T & 0 & D^T & -\gamma I_m \end{array}\right].$$

It can be shown that if $\lambda E - A$ has no purely imaginary eigenvalue and $\gamma > \inf_{\omega\in\mathbb{R}} \sigma_{\max}(G(i\omega))$, then $\|G\|_{\mathcal{H}_\infty} \geq \gamma$ if and only if $\lambda\mathcal{E} - \mathcal{A}(\gamma)$ has purely imaginary eigenvalues. In this way, we can again use an iterative scheme to update the value of γ until a desired accuracy for the $\mathcal{H}_\infty$-norm is achieved.

3. THEORY AND ALGORITHM DESCRIPTION

In this section, we briefly describe the theory behind the algorithms that we will use. We refer to Benner et al. [2002, 2007] for a detailed analysis of the algorithms. We consider complex and real problems separately since there are significant differences in the theory. We also distinguish the cases of unfactored and factored skew-Hamiltonian matrices $\mathcal{S}$. This is motivated by the fact that, in certain cases, a skew-Hamiltonian matrix $\mathcal{S}$ admits a factorization

$$\mathcal{S} = \mathcal{J}\mathcal{Z}^H\mathcal{J}^T\mathcal{Z}. \tag{10}$$

For example, if $\mathcal{S} = [\begin{smallmatrix} E & 0 \\ 0 & E^H \end{smallmatrix}]$, then $\mathcal{Z} = [\begin{smallmatrix} I & 0 \\ 0 & E^H \end{smallmatrix}]$. The factorization in Equation (10) can be understood as a Cholesky-like decomposition of $\mathcal{S}$ with respect to the indefinite inner product $\langle x, y\rangle := x^H\mathcal{J}y$, since $\mathcal{J}\mathcal{Z}^H\mathcal{J}^T$ is the adjoint of $\mathcal{Z}$ with respect to $\langle\cdot,\cdot\rangle$. We also say that a skew-Hamiltonian matrix $\mathcal{S}$ is *$\mathcal{J}$-semidefinite* if it admits a factorization of the form in Equation (10). Hence, in our implementation, we distinguish those cases that the full matrix $\mathcal{S}$ or just its "Cholesky factor" $\mathcal{Z}$ is given. In all cases, we apply an embedding strategy to the matrix pencil $\lambda\mathcal{S} - \mathcal{H}$ to ensure the existence of a structured Schur form.

3.1. The Complex Case

Let $\lambda\mathcal{S} - \mathcal{H} \in \mathbb{C}[\lambda]^{2n\times 2n}$ be a given skew-Hamiltonian/Hamiltonian matrix pencil with $\mathcal{J}$-semidefinite skew-Hamiltonian part $\mathcal{S} = \mathcal{J}\mathcal{Z}^H\mathcal{J}^T\mathcal{Z}$. We split the skew-Hamiltonian matrix $\mathrm{i}\mathcal{H} =: \mathcal{N} = \mathcal{N}_1 + \mathrm{i}\mathcal{N}_2$, where $\mathcal{N}_1$ is real skew-Hamiltonian and $\mathcal{N}_2$ is real Hamiltonian, that is:

$$\mathcal{N}_1 = \begin{bmatrix} F_1 & G_1 \\ H_1 & F_1^T \end{bmatrix}, \quad G_1 = -G_1^T, \quad H_1 = -H_1^T,$$

$$\mathcal{N}_2 = \begin{bmatrix} F_2 & G_2 \\ H_2 & -F_2^T \end{bmatrix}, \quad G_2 = G_2^T, \quad H_2 = H_2^T,$$

and $F_j, G_j, H_j \in \mathbb{R}^{n\times n}$ for $j = 1, 2$. We define the matrices

$$\mathcal{Y}_c = \frac{\sqrt{2}}{2}\begin{bmatrix} I_{2n} & \mathrm{i}I_{2n} \\ I_{2n} & -\mathrm{i}I_{2n} \end{bmatrix}, \quad \mathcal{P} = \begin{bmatrix} I_n & 0 & 0 & 0 \\ 0 & 0 & I_n & 0 \\ 0 & I_n & 0 & 0 \\ 0 & 0 & 0 & I_n \end{bmatrix}, \quad \mathcal{X}_c = \mathcal{Y}_c\mathcal{P}. \tag{11}$$

When denoting by $\overline{M}$ the complex conjugate matrix of M and performing the embedding $\mathcal{B}_\mathcal{N} := \mathrm{diag}(\mathcal{N}, \overline{\mathcal{N}})$ we obtain that

$$\mathcal{B}_\mathcal{N}^c := \mathcal{X}_c^H\mathcal{B}_\mathcal{N}\mathcal{X}_c = \left[\begin{array}{cc|cc} F_1 & -F_2 & G_1 & -G_2 \\ F_2 & F_1 & G_2 & G_1 \\ \hline H_1 & -H_2 & F_1^T & F_2^T \\ H_2 & H_1 & -F_2^T & F_1^T \end{array}\right] \tag{12}$$

is a real $4n \times 4n$ skew-Hamiltonian matrix. Similarly, we define

$$\mathcal{B}_\mathcal{Z} := \begin{bmatrix} \mathcal{Z} & 0 \\ 0 & \overline{\mathcal{Z}} \end{bmatrix}, \quad \mathcal{B}_\mathcal{T} := \begin{bmatrix} \mathcal{J}\mathcal{Z}^H\mathcal{J}^T & 0 \\ 0 & \overline{\mathcal{J}\mathcal{Z}^H\mathcal{J}^T} \end{bmatrix}, \quad \mathcal{B}_\mathcal{S} := \begin{bmatrix} \mathcal{S} & 0 \\ 0 & \overline{\mathcal{S}} \end{bmatrix} = \mathcal{B}_\mathcal{T}\mathcal{B}_\mathcal{Z}.$$

It can be shown that

$$\mathcal{B}_\mathcal{Z}^c := \mathcal{X}_c^H\mathcal{B}_\mathcal{Z}\mathcal{X}_c, \quad \mathcal{B}_\mathcal{T}^c := \mathcal{X}_c^H\mathcal{B}_\mathcal{T}\mathcal{X}_c, \quad \mathcal{B}_\mathcal{S}^c := \mathcal{X}_c^H\mathcal{B}_\mathcal{S}\mathcal{X}_c \tag{13}$$

are all real. Hence,

$$\lambda\mathcal{B}^c_{\mathcal{S}} - \mathcal{B}^c_{\mathcal{N}} = \mathcal{X}_c^H(\lambda\mathcal{B}_{\mathcal{S}} - \mathcal{B}_{\mathcal{N}})\mathcal{X}_c = \mathcal{X}_c^H\left(\begin{bmatrix}\lambda\mathcal{S}-\mathcal{N} & 0\\ 0 & \lambda\overline{\mathcal{S}}-\overline{\mathcal{N}}\end{bmatrix}\right)\mathcal{X}_c$$

is a real $4n \times 4n$ skew-Hamiltonian/skew-Hamiltonian matrix pencil. To compute the eigenvalues of this matrix pencil, we can compute the structured decomposition of the following theorem [Benner et al. 2002].

THEOREM 3.1. *Let $\lambda\mathcal{S} - \mathcal{N} \in \mathbb{R}[\lambda]^{2n\times 2n}$ be a regular skew-Hamiltonian/skew-Hamiltonian matrix pencil with $\mathcal{S} = \mathcal{J}\mathcal{Z}^T\mathcal{J}^T\mathcal{Z}$. Then there exist a real orthogonal matrix $\mathcal{Q} \in \mathbb{R}^{2n\times 2n}$ and a real orthogonal symplectic matrix $\mathcal{U} \in \mathbb{R}^{2n\times 2n}$ such that*

$$\begin{aligned}\mathcal{U}^T\mathcal{Z}\mathcal{Q} &= \begin{bmatrix} Z_{11} & Z_{12}\\ 0 & Z_{22}\end{bmatrix},\\ \mathcal{J}\mathcal{Q}^T\mathcal{J}^T\mathcal{N}\mathcal{Q} &= \begin{bmatrix} N_{11} & N_{12}\\ 0 & N_{11}^T\end{bmatrix},\end{aligned} \tag{14}$$

where Z_{11} and Z_{22}^T are upper triangular, N_{11} is upper quasi-triangular, and N_{12} is skew-symmetric. Moreover,

$$\begin{aligned}\mathcal{J}\mathcal{Q}^T\mathcal{J}^T(\lambda\mathcal{S}-\mathcal{N})\mathcal{Q} &= \lambda\begin{bmatrix} Z_{22}^TZ_{11} & Z_{22}^TZ_{12} - Z_{12}^TZ_{22}\\ 0 & Z_{11}^TZ_{22}\end{bmatrix} - \begin{bmatrix} N_{11} & N_{12}\\ 0 & N_{11}^T\end{bmatrix}\\ &=: \lambda\begin{bmatrix} S_{11} & S_{12}\\ 0 & S_{11}^T\end{bmatrix} - \begin{bmatrix} N_{11} & N_{12}\\ 0 & N_{11}^T\end{bmatrix}\end{aligned} \tag{15}$$

is a $\mathcal{J}$-congruent skew-Hamiltonian/skew-Hamiltonian matrix pencil.

PROOF. See Benner et al. [2002]. □

By defining

$$\mathcal{B}_{\mathcal{H}} = \begin{bmatrix}\mathcal{H} & 0\\ 0 & -\overline{\mathcal{H}}\end{bmatrix}, \quad \mathcal{B}^c_{\mathcal{H}} = \mathcal{X}_c^H\mathcal{B}_{\mathcal{H}}\mathcal{X}_c,$$

and using Theorem 3.1, we can compute factorizations

$$\begin{aligned}\widetilde{\mathcal{B}}^c_{\mathcal{Z}} &:= \mathcal{U}^T\mathcal{B}^c_{\mathcal{Z}}\mathcal{Q} = \begin{bmatrix}\mathcal{Z}_{11} & \mathcal{Z}_{12}\\ 0 & \mathcal{Z}_{22}\end{bmatrix},\\ \widetilde{\mathcal{B}}^c_{\mathcal{H}} &:= \mathcal{J}\mathcal{Q}^T\mathcal{J}^T\mathcal{B}^c_{\mathcal{H}}\mathcal{Q} = \mathcal{J}\mathcal{Q}^T\mathcal{J}^T\left(-\mathrm{i}\mathcal{B}^c_{\mathcal{N}}\right)\mathcal{Q} = -\mathrm{i}\widetilde{\mathcal{B}}^c_{\mathcal{N}} = \begin{bmatrix}-\mathrm{i}\mathcal{N}_{11} & -\mathrm{i}\mathcal{N}_{12}\\ 0 & -(-\mathrm{i}\mathcal{N}_{11})^H\end{bmatrix},\end{aligned}$$

where $\lambda\widetilde{\mathcal{B}}^c_{\mathcal{S}} - \widetilde{\mathcal{B}}^c_{\mathcal{H}} = \mathcal{J}\mathcal{Q}^T\mathcal{J}^T(\lambda\mathcal{B}^c_{\mathcal{S}} - \mathcal{B}^c_{\mathcal{H}})\mathcal{Q}$ are $\mathcal{J}$-congruent complex skew-Hamiltonian/Hamiltonian matrix pencils and $\lambda\widetilde{\mathcal{B}}^c_{\mathcal{S}} - \widetilde{\mathcal{B}}^c_{\mathcal{H}}$ is in a structured quasi-triangular form. Then, the structured Schur form can be obtained by further triangularizing the diagonal 2×2 blocks of $\lambda\widetilde{\mathcal{B}}^c_{\mathcal{S}} - \widetilde{\mathcal{B}}^c_{\mathcal{H}}$ via a $\mathcal{J}$-congruence transformation. From the symmetry of the eigenvalues, it follows that $\Lambda(\mathcal{S},\mathcal{H}) = \Lambda(\mathcal{Z}_{22}^H\mathcal{Z}_{11}, -\mathrm{i}\mathcal{N}_{11})$. Now we can reorder the eigenvalues of $\lambda\widetilde{\mathcal{B}}^c_{\mathcal{S}} - \widetilde{\mathcal{B}}^c_{\mathcal{H}}$ to the top in order to compute the desired deflating subspaces (corresponding to the eigenvalues with negative real parts). The following theorem makes statements about the deflating subspaces [Benner et al. 2002].

THEOREM 3.2. *Let $\lambda\mathcal{S} - \mathcal{H} \in \mathbb{C}[\lambda]^{2n\times 2n}$ be a skew-Hamiltonian/Hamiltonian matrix pencil with $\mathcal{J}$-semidefinite skew-Hamiltonian matrix $\mathcal{S} = \mathcal{J}\mathcal{Z}^H\mathcal{J}^T\mathcal{Z}$. Consider* *the extended matrices* $\mathcal{B}_{\mathcal{Z}} = \operatorname{diag}(\mathcal{Z}, \overline{\mathcal{Z}})$, $\mathcal{B}_{\mathcal{T}} = \operatorname{diag}(\mathcal{J}\mathcal{Z}^H\mathcal{J}^T, \overline{\mathcal{J}\mathcal{Z}^H\mathcal{J}^T})$, $\mathcal{B}_{\mathcal{S}} = \mathcal{B}_{\mathcal{T}}\mathcal{B}_{\mathcal{Z}} = \operatorname{diag}(\mathcal{S}, \overline{\mathcal{S}})$, $\mathcal{B}_{\mathcal{H}} = \operatorname{diag}(\mathcal{H}, -\overline{\mathcal{H}})$. *Let* $\mathcal{U}$, $\mathcal{V}$, $\mathcal{W}$ *be unitary matrices such that*

$$\mathcal{U}^H\mathcal{B}_{\mathcal{Z}}\mathcal{V} = \begin{bmatrix} \mathcal{Z}_{11} & \mathcal{Z}_{12} \\ 0 & \mathcal{Z}_{22} \end{bmatrix} =: \mathcal{R}_{\mathcal{Z}},$$

$$\mathcal{W}^H\mathcal{B}_{\mathcal{T}}\mathcal{U} = \begin{bmatrix} \mathcal{T}_{11} & \mathcal{T}_{12} \\ 0 & \mathcal{T}_{22} \end{bmatrix} =: \mathcal{R}_{\mathcal{T}},$$

$$\mathcal{W}^H\mathcal{B}_{\mathcal{H}}\mathcal{V} = \begin{bmatrix} \mathcal{H}_{11} & \mathcal{H}_{12} \\ 0 & \mathcal{H}_{22} \end{bmatrix} =: \mathcal{R}_{\mathcal{H}},$$

where $\Lambda_-(\mathcal{B}_{\mathcal{S}}, \mathcal{B}_{\mathcal{H}}) \subset \Lambda(\mathcal{T}_{11}\mathcal{Z}_{11}, \mathcal{H}_{11})$ *and* $\Lambda(\mathcal{T}_{11}\mathcal{Z}_{11}, \mathcal{H}_{11}) \cap \Lambda_+(\mathcal{B}_{\mathcal{S}}, \mathcal{B}_{\mathcal{H}}) = \emptyset$. *Here,* $\mathcal{Z}_{11}, \mathcal{T}_{11}, \mathcal{H}_{11} \in \mathbb{C}^{m\times m}$. *Suppose* $\Lambda_-(\mathcal{S}, \mathcal{H})$ *contains* p *eigenvalues. If* $\left[\begin{smallmatrix} V_1 \\ V_2 \end{smallmatrix}\right] \in \mathbb{C}^{4n\times m}$ *are the first* m *columns of* $\mathcal{V}$, $2p \le m \le 2n - 2p$, *then there are subspaces* $\mathbb{L}_1$ *and* $\mathbb{L}_2$ *such that*

$$\begin{aligned} \operatorname{range} V_1 &= \operatorname{Defl}_-(\mathcal{S}, \mathcal{H}) + \mathbb{L}_1, \quad \mathbb{L}_1 \subseteq \operatorname{Defl}_0(\mathcal{S}, \mathcal{H}) + \operatorname{Defl}_\infty(\mathcal{S}, \mathcal{H}), \\ \operatorname{range} \overline{V_2} &= \operatorname{Defl}_+(\mathcal{S}, \mathcal{H}) + \mathbb{L}_2, \quad \mathbb{L}_2 \subseteq \operatorname{Defl}_0(\mathcal{S}, \mathcal{H}) + \operatorname{Defl}_\infty(\mathcal{S}, \mathcal{H}). \end{aligned}$$

If $\Lambda(\mathcal{T}_{11}\mathcal{Z}_{11}, \mathcal{H}_{11}) = \Lambda_-(\mathcal{B}_{\mathcal{S}}, \mathcal{B}_{\mathcal{H}})$, *and* $\left[\begin{smallmatrix} U_1 \\ U_2 \end{smallmatrix}\right]$, $\left[\begin{smallmatrix} W_1 \\ W_2 \end{smallmatrix}\right]$ *are the first* m *columns of* $\mathcal{U}$, $\mathcal{W}$, *respectively, then there exist unitary matrices* Q_U, Q_V, Q_W *such that*

$$\begin{aligned} U_1 &= [P_U^- \ \ 0]Q_U, \quad U_2 = [0 \ \ P_U^+]Q_U, \\ V_1 &= [P_V^- \ \ 0]Q_V, \quad V_2 = [0 \ \ P_V^+]Q_V, \\ W_1 &= [P_W^- \ \ 0]Q_W, \quad W_2 = [0 \ \ P_W^+]Q_W, \end{aligned}$$

and the columns of P_V^- *and* $\overline{P_V^+}$ *form orthogonal bases of* $\operatorname{Defl}_-(\mathcal{S}, \mathcal{H})$ *and* $\operatorname{Defl}_+(\mathcal{S}, \mathcal{H})$, *respectively. Moreover, the matrices* P_U^-, P_U^+, P_W^-, *and* P_W^+ *have orthonormal columns and the following relations are satisfied:*

$$\begin{aligned} \mathcal{Z}P_V^- &= P_U^-\widetilde{Z}_{11}, \quad \mathcal{J}\mathcal{Z}^H\mathcal{J}^T P_U^- = P_W^-\widetilde{T}_{11}, \quad \mathcal{H}P_V^- = P_W^-\widetilde{H}_{11}, \\ \mathcal{Z}\overline{P_V^+} &= \overline{P_U^+}\,\overline{\widetilde{Z}_{22}}, \quad \mathcal{J}\mathcal{Z}^H\mathcal{J}^T\overline{P_U^+} = \overline{P_W^+}\,\overline{\widetilde{T}_{22}}, \quad \mathcal{H}\overline{P_V^+} = -\overline{P_W^+}\,\overline{\widetilde{H}_{22}}. \end{aligned}$$

Here, $\widetilde{Z}_{kk}$, $\widetilde{T}_{kk}$, *and* $\widetilde{H}_{kk}$, $k = 1, 2$, *satisfy* $\Lambda(\widetilde{T}_{11}\widetilde{Z}_{11}, \widetilde{H}_{11}) = \Lambda(\widetilde{T}_{22}\widetilde{Z}_{22}, \widetilde{H}_{22}) = \Lambda_-(\mathcal{S}, \mathcal{H})$.

PROOF. See Benner et al. [2002]. □

If the matrix $\mathcal{S}$ is not given in factored form, we can use the following algorithm for the computation of the deflating subspaces [Benner et al. 2002]. The other algorithms are similar; however, for brevity we refer to Benner et al. [2002, 2007].

Now we present the algorithm for the computation of the structured matrix factorization in Equation (16).

Now, the eigenvalues of $\lambda\mathcal{S} - \mathcal{N}$ are determined by the diagonal 1×1 and 2×2 blocks of S_{11} and N_{11}. Next, we consider an eigenvalue reordering routine in order to move the eigenvalues with negative real part of a skew-Hamiltonian/Hamiltonian pencil to the leading principal subpencil.

3.2. The Real Case

We also briefly review the theory for the real case, which has some significant differences compared to the complex case. For a detailed description, we refer to Benner

ALGORITHM 1: Computation of Stable Deflating Subspaces of Complex Skew-Hamiltonian/Hamiltonian Matrix Pencils in Unfactored Form.

```
Input: A skew-Hamiltonian/Hamiltonian matrix pencil $\lambda\mathcal{S} - \mathcal{H} \in \mathbb{C}[\lambda]^{2n\times 2n}$.
Output: Structured Schur form of the extended skew-Hamiltonian/Hamiltonian matrix pencil
    $\lambda\mathcal{B}_{\mathcal{S}}^{c} - \mathcal{B}_{\mathcal{H}}^{c}$, eigenvalues of $\lambda\mathcal{S} - \mathcal{H}$, orthonormal basis $P_V^-$ of the deflating subspace
    $\mathrm{Defl}_-(\mathcal{S}, \mathcal{H})$, as in Theorem 3.2.
1: Set $\mathcal{N} = \mathrm{i}\mathcal{H}$ and determine the matrices $\mathcal{B}_{\mathcal{S}}^{c}$, $\mathcal{B}_{\mathcal{N}}^{c}$ as in Equations (13) and (12), respectively.
   Perform Algorithm 2 to compute the factorization
   $$\begin{aligned}\widehat{\mathcal{B}}_{\mathcal{S}}^{c} &= \mathcal{J}\mathcal{Q}^T\mathcal{J}^T\mathcal{B}_{\mathcal{S}}^{c}\mathcal{Q} = \begin{bmatrix}\mathcal{S}_{11} & \mathcal{S}_{12}\\ 0 & \mathcal{S}_{11}^T\end{bmatrix},\\ \widehat{\mathcal{B}}_{\mathcal{N}}^{c} &= \mathcal{J}\mathcal{Q}^T\mathcal{J}^T\mathcal{B}_{\mathcal{N}}^{c}\mathcal{Q} = \begin{bmatrix}\mathcal{N}_{11} & \mathcal{N}_{12}\\ 0 & \mathcal{N}_{11}^T\end{bmatrix},\end{aligned} \qquad (16)$$
   where $\mathcal{Q}$ is real orthogonal, $\mathcal{S}_{11}$ is upper triangular and $\mathcal{N}_{11}$ is upper quasi-triangular.
2: Apply the QZ algorithm [Golub and Van Loan 1996] to the $2 \times 2$ diagonal blocks of the
   matrix pencil $\lambda\mathcal{S}_{11} - \mathcal{N}_{11}$ to determine unitary matrices $\mathcal{Q}_1$, $\mathcal{Q}_2$ such that
   $\mathcal{Q}_2^H\mathcal{S}_{11}\mathcal{Q}_1$, $\mathcal{Q}_2^H\mathcal{N}_{11}\mathcal{Q}_1$ are both upper triangular. Define $\widehat{\mathcal{Q}} := \mathrm{diag}(\mathcal{Q}_1, \mathcal{Q}_2)$ and set
   $$\widetilde{\mathcal{B}}_{\mathcal{S}}^{c} = \mathcal{J}\widehat{\mathcal{Q}}^H\mathcal{J}^T\widehat{\mathcal{B}}_{\mathcal{S}}^{c}\widehat{\mathcal{Q}}, \quad \widetilde{\mathcal{B}}_{\mathcal{N}}^{c} = \mathcal{J}\widehat{\mathcal{Q}}^H\mathcal{J}^T\widehat{\mathcal{B}}_{\mathcal{N}}^{c}\widehat{\mathcal{Q}}.$$
3: Use Algorithm 3 to determine a unitary matrix $\widetilde{\mathcal{Q}}$ such that
   $$\begin{aligned}\mathcal{J}\widetilde{\mathcal{Q}}^H\mathcal{J}^T\widetilde{\mathcal{B}}_{\mathcal{S}}^{c}\widetilde{\mathcal{Q}} &= \begin{bmatrix}\widetilde{\mathcal{S}}_{11} & \widetilde{\mathcal{S}}_{12}\\ 0 & \widetilde{\mathcal{S}}_{11}^H\end{bmatrix},\\ \mathcal{J}\widetilde{\mathcal{Q}}^H\mathcal{J}^T\left(-\mathrm{i}\widetilde{\mathcal{B}}_{\mathcal{N}}^{c}\right)\widetilde{\mathcal{Q}} &= \begin{bmatrix}\widetilde{\mathcal{H}}_{11} & \widetilde{\mathcal{H}}_{12}\\ 0 & -\widetilde{\mathcal{H}}_{11}^H\end{bmatrix},\end{aligned}$$
   where $\widetilde{\mathcal{S}}_{11}$, $\widetilde{\mathcal{H}}_{11}$ are upper triangular such that $\Lambda_-\left(\widetilde{\mathcal{B}}_{\mathcal{S}}^{c}, -\mathrm{i}\widetilde{\mathcal{B}}_{\mathcal{N}}^{c}\right)$ is containedin the spectrum of
   the $2p \times 2p$ leading principal subpencil of $\lambda\widetilde{\mathcal{S}}_{11} - \widetilde{\mathcal{H}}_{11}$.
4: Set $V = [I_{2n} \;\; 0]\,\mathcal{X}_c\mathcal{Q}\widehat{\mathcal{Q}}\widetilde{\mathcal{Q}}\left[\begin{smallmatrix}I_{2p}\\ 0\end{smallmatrix}\right]$ and compute $P_V^-$, an orthogonal basis of range $V$, using any
   numerically stable orthogonalization scheme.
```

et al. [2007]. Let $\lambda\mathcal{S} - \mathcal{H} \in \mathbb{R}[\lambda]^{2n\times 2n}$ be a skew-Hamiltonian/Hamiltonian matrix pencil with $\mathcal{J}$-semidefinite skew-Hamiltonian part $\mathcal{S} = \mathcal{J}\mathcal{Z}^T\mathcal{J}^T\mathcal{Z}$ where $\mathcal{Z} = \left[\begin{smallmatrix}Z_{11} & Z_{12}\\ Z_{21} & Z_{22}\end{smallmatrix}\right]$, $\mathcal{H} = \left[\begin{smallmatrix}F & G\\ H & -F^T\end{smallmatrix}\right]$. We introduce the orthogonal matrices

$$\mathcal{Y}_r = \frac{\sqrt{2}}{2}\begin{bmatrix}I_{2n} & I_{2n}\\ -I_{2n} & I_{2n}\end{bmatrix}, \quad \mathcal{X}_r = \mathcal{Y}_r\mathcal{P}$$

with $\mathcal{P}$ as in Equation (11). Now we define the double-sized matrices

$$\begin{aligned}\mathcal{B}_{\mathcal{Z}} &:= \begin{bmatrix}\mathcal{Z} & 0\\ 0 & \mathcal{Z}\end{bmatrix},\\ \mathcal{B}_{\mathcal{T}} &:= \begin{bmatrix}\mathcal{J}\mathcal{Z}^T\mathcal{J}^T & 0\\ 0 & \mathcal{J}\mathcal{Z}^T\mathcal{J}^T\end{bmatrix} = \begin{bmatrix}\mathcal{J} & 0\\ 0 & \mathcal{J}\end{bmatrix}\mathcal{B}_{\mathcal{Z}}^T\begin{bmatrix}\mathcal{J} & 0\\ 0 & \mathcal{J}\end{bmatrix}^T,\end{aligned}$$

$$\begin{aligned}\mathcal{B}_{\mathcal{S}} &:= \begin{bmatrix}\mathcal{S} & 0\\ 0 & \mathcal{S}\end{bmatrix} = \mathcal{B}_{\mathcal{T}}\mathcal{B}_{\mathcal{Z}},\\ \mathcal{B}_{\mathcal{H}} &:= \begin{bmatrix}\mathcal{H} & 0\\ 0 & -\mathcal{H}\end{bmatrix}.\end{aligned}$$

ALGORITHM 2: Computation of a Structured Matrix Factorization for Real Skew-Hamiltonian/Skew-Hamiltonian Matrix Pencils in Unfactored Form.

```
Input: A skew-Hamiltonian/skew-Hamiltonian matrix pencil $\lambda\mathcal{S} - \mathcal{N} \in \mathbb{R}[\lambda]^{2n\times 2n}$.
Output: A real orthogonal matrix $\mathcal{Q}$ and the structured factorization in Equation (15).
1: Set $\mathcal{Q} = I_{2n}$. Reduce $\mathcal{S}$ to skew-Hamiltonian triangular form, i.e., determine an orthogonal
   matrix $\mathcal{Q}_1$ such that
      $$\mathcal{S} := \mathcal{J}\mathcal{Q}_1^T\mathcal{J}^T\mathcal{S}\mathcal{Q}_1 = \begin{bmatrix} S_{11} & S_{12} \\ 0 & S_{11}^T \end{bmatrix}$$
   with an upper triangular matrix $S_{11}$. Update $\mathcal{N} := \mathcal{J}\mathcal{Q}_1^T\mathcal{J}^T\mathcal{N}\mathcal{Q}_1$, $\mathcal{Q} := \mathcal{Q}\mathcal{Q}_1$. This step is
   performed by applying a sequence of Householder reflections and Givens rotations in a
   specific order, see Benner et al. [2002] for details.
2: Reduce $\mathcal{N}$ to skew-Hamiltonian Hessenberg form. Determine an orthogonal matrix $\mathcal{Q}_1$ such
   that
      $$\mathcal{S} : = \mathcal{J}\mathcal{Q}_1^T\mathcal{J}^T\mathcal{S}\mathcal{Q}_1 = \begin{bmatrix} S_{11} & S_{12} \\ 0 & S_{11}^T \end{bmatrix},$$
      $$\mathcal{N} : = \mathcal{J}\mathcal{Q}_1^T\mathcal{J}^T\mathcal{N}\mathcal{Q}_1 = \begin{bmatrix} N_{11} & N_{12} \\ 0 & N_{11}^T \end{bmatrix},$$
   where $S_{11}$ is upper triangular and $N_{11}$ is upper Hessenberg. Update $\mathcal{Q} := \mathcal{Q}\mathcal{Q}_1$. This step is
   performed by applying an appropriate sequence of Givens rotations to annihilate the
   elements in $\mathcal{N}$ in a specific order without destroying the structure of $\mathcal{S}$, for details see
   Benner et al. [2002].
3: Apply the QZ algorithm to the matrix pencil $\lambda S_{11} - N_{11}$ to determine orthogonal matrices
   $Q_1$ and $Q_2$ such that $Q_2^T S_{11} Q_1$ is upper triangular and $Q_2^T N_{11} Q_1$ is upper quasi-triangular.
   Set $\mathcal{Q}_1 := \mathrm{diag}(Q_1, Q_2)$ and update $\mathcal{S} := \mathcal{J}\mathcal{Q}_1^T\mathcal{J}^T\mathcal{S}\mathcal{Q}_1$, $\mathcal{N} := \mathcal{J}\mathcal{Q}_1^T\mathcal{J}^T\mathcal{N}\mathcal{Q}_1$, $\mathcal{Q} := \mathcal{Q}\mathcal{Q}_1$.
```

Furthermore, we define

$$\begin{aligned}
\mathcal{B}_{\mathcal{Z}}^r &: = \mathcal{X}_r^T\mathcal{B}_{\mathcal{Z}}\mathcal{X}_r = \begin{bmatrix} Z_{11} & 0 & Z_{12} & 0 \\ 0 & Z_{11} & 0 & Z_{12} \\ Z_{21} & 0 & Z_{22} & 0 \\ 0 & Z_{21} & 0 & Z_{22} \end{bmatrix}, \\
\mathcal{B}_{\mathcal{T}}^r &: = \mathcal{X}_r^T\mathcal{B}_{\mathcal{T}}\mathcal{X}_r = \mathcal{J}\left(\mathcal{B}_{\mathcal{Z}}^r\right)^T\mathcal{J}^T, \\
\mathcal{B}_{\mathcal{S}}^r &: = \mathcal{X}_r^T\mathcal{B}_{\mathcal{S}}\mathcal{X}_r = \mathcal{J}\left(\mathcal{B}_{\mathcal{Z}}^r\right)^T\mathcal{J}^T\mathcal{B}_{\mathcal{Z}}^r, \\
\mathcal{B}_{\mathcal{H}}^r &: = \mathcal{X}_r^T\mathcal{B}_{\mathcal{H}}\mathcal{X}_r = \left[\begin{array}{cc|cc} 0 & F & 0 & G \\ F & 0 & G & 0 \\ \hline 0 & H & 0 & -F^T \\ H & 0 & -F^T & 0 \end{array}\right].
\end{aligned}$$

It can be easily observed that the $4n \times 4n$ matrix pencil $\lambda\mathcal{B}_{\mathcal{S}}^r - \mathcal{B}_{\mathcal{H}}^r$ is again real skew-Hamiltonian/Hamiltonian. For the computation of the eigenvalues of $\lambda\mathcal{S} - \mathcal{H}$, we apply the following structured matrix factorization, which is also often referred to as *generalized symplectic URV decomposition* [Benner et al. 2007].

THEOREM 3.3. *Let $\lambda\mathcal{S} - \mathcal{H} \in \mathbb{R}[\lambda]^{2n\times 2n}$ be a skew-Hamiltonian/Hamiltonian matrix pencil with $\mathcal{S} = \mathcal{J}\mathcal{Z}^T\mathcal{J}^T\mathcal{Z}$. Then there exist orthogonal matrices $\mathcal{Q}_1$, $\mathcal{Q}_2$ and orthogonal*

ALGORITHM 3: Eigenvalue Reordering for Complex Skew-Hamiltonian/Hamiltonian Matrix Pencils in Unfactored Form.

```
Input: A regular skew-Hamiltonian/Hamiltonian matrix pencil $\lambda\mathcal{S} - \mathcal{H} \in \mathbb{C}[\lambda]^{2n\times 2n}$ of the form
    $\mathcal{S} = [\begin{smallmatrix} S & W \\ 0 & S^H \end{smallmatrix}]$, $\mathcal{H} = [\begin{smallmatrix} H & 0 \\ D & -H^H \end{smallmatrix}]$, with upper triangular $S$, $H$.
Output: A unitary matrix $\mathcal{Q}$ and the transformed matrices $\mathcal{J}\mathcal{Q}^H\mathcal{J}^T\mathcal{S}\mathcal{Q}$, $\mathcal{J}\mathcal{Q}^H\mathcal{J}^T\mathcal{H}\mathcal{Q}$ which
    have still the same triangular form as $\mathcal{S}$ and $\mathcal{H}$, respectively, but the eigenvalues in
    $\Lambda_-(\mathcal{S},\mathcal{H})$ are reordered such that they occur in the leading principal subpencil of
    $\mathcal{J}\mathcal{Q}^H\mathcal{J}^T(\lambda\mathcal{S} - \mathcal{H})\mathcal{Q}$.
1: Set $\mathcal{Q} = I_{2n}$. Reorder the eigenvalues in the subpencil $\lambda S - H$.
    a) Determine unitary matrices $Q_1$, $Q_2$ such that $S := Q_2^H S Q_1$, $H := Q_2^H H Q_1$ are still upper
       triangular but the $m_-$ eigenvalues with negative real part are reordered to the top of
       $\lambda S - H$. Set $\mathcal{Q}_1 := \mathrm{diag}(Q_1, Q_2)$ and update $\mathcal{Q} := \mathcal{Q}\mathcal{Q}_1$.
    b) Determine unitary matrices $Q_1$, $Q_2$ such that $S := Q_2^H S Q_1$, $H := Q_2^H H Q_1$ are still upper
       triangular but the $m_+$ eigenvalues with positive real part are reordered to the bottom of
       $\lambda S - H$. Set $\mathcal{Q}_1 := \mathrm{diag}(Q_1, Q_2)$ and update $\mathcal{Q} := \mathcal{Q}\mathcal{Q}_1$.
2: Reorder the remaining $n - m_+ + 1$ eigenvalues with negative real parts which are now in the
   bottom right subpencil of $\lambda\mathcal{S} - \mathcal{H}$. Determine a unitary matrix $\mathcal{Q}_1$ such that the eigenvalues
   of the top left subpencil of $\lambda\mathcal{S} - \mathcal{H}$ with positive real parts and those of the bottom right
   subpencil of $\lambda\mathcal{S} - \mathcal{H}$ with negative real parts are interchanged. Update $\mathcal{Q} := \mathcal{Q}\mathcal{Q}_1$.
```

symplectic matrices $\mathcal{U}_1$, $\mathcal{U}_2$ such that

$$\begin{aligned} \mathcal{Q}_1^T(\mathcal{J}\mathcal{Z}^T\mathcal{J}^T)\mathcal{U}_1 &= \begin{bmatrix} T_{11} & T_{12} \\ 0 & T_{22} \end{bmatrix}, \\ \mathcal{U}_2^T\mathcal{Z}\mathcal{Q}_2 &= \begin{bmatrix} Z_{11} & Z_{12} \\ 0 & Z_{22} \end{bmatrix}, \\ \mathcal{Q}_1^T\mathcal{H}\mathcal{Q}_2 &= \begin{bmatrix} H_{11} & H_{12} \\ 0 & H_{22} \end{bmatrix}, \end{aligned} \tag{17}$$

with the formal matrix product $T_{11}^{-1}H_{11}Z_{11}^{-1}Z_{22}^{-T}H_{22}^TT_{22}^{-T}$ in real periodic Schur form [Bojanczyk et al. 1992; Hench and Laub 1994], where T_{11}, Z_{11}, H_{11}, T_{22}^T, Z_{22}^T are upper triangular and H_{22}^T is upper quasi-triangular.

Proof. The proof is constructive; see Benner et al. [2007]. □

By using Theorem 3.3 (with the same notation), we get the following factorization of the embedded matrix pencil $\lambda\mathcal{B}_\mathcal{S}^r - \mathcal{B}_\mathcal{H}^r$ with a factored matrix $\mathcal{B}_\mathcal{S}^r$. We can compute an orthogonal matrix $\widetilde{\mathcal{Q}}$ and an orthogonal symplectic matrix $\widetilde{\mathcal{U}}$ such that

$$\begin{aligned} \widetilde{\mathcal{U}}^T\mathcal{B}_\mathcal{Z}^r\widetilde{\mathcal{Q}} &= \left[\begin{array}{cc|cc} T_{22}^T & 0 & -T_{12}^T & 0 \\ 0 & Z_{11} & 0 & Z_{12} \\ \hline 0 & 0 & T_{11}^T & 0 \\ 0 & 0 & 0 & Z_{22} \end{array}\right] =: \begin{bmatrix} \widetilde{\mathcal{Z}}_{11} & \widetilde{\mathcal{Z}}_{12} \\ 0 & \widetilde{\mathcal{Z}}_{22} \end{bmatrix}, \\ \mathcal{J}\widetilde{\mathcal{Q}}^T\mathcal{J}^T\mathcal{B}_\mathcal{H}^r\widetilde{\mathcal{Q}} &= \left[\begin{array}{cc|cc} 0 & H_{11} & 0 & H_{12} \\ -H_{22}^T & 0 & H_{12} & 0 \\ \hline 0 & 0 & 0 & H_{22} \\ 0 & 0 & -H_{11}^T & 0 \end{array}\right] =: \begin{bmatrix} \widetilde{\mathcal{H}}_{11} & \widetilde{\mathcal{H}}_{12} \\ 0 & -\widetilde{\mathcal{H}}_{11}^T \end{bmatrix}, \end{aligned} \tag{18}$$

where $\widetilde{\mathcal{Q}} = \mathcal{P}^T \left[\begin{smallmatrix} \mathcal{J}\mathcal{Q}_1\mathcal{J}^T & 0 \\ 0 & \mathcal{Q}_2 \end{smallmatrix}\right] \mathcal{P}$, $\widetilde{\mathcal{U}} = \mathcal{P}^T \left[\begin{smallmatrix} \mathcal{U}_1 & 0 \\ 0 & \mathcal{U}_2 \end{smallmatrix}\right] \mathcal{P}$. From the condensed form in Equation (18), we can immediately get the eigenvalues of $\lambda\mathcal{S} - \mathcal{H}$ as

$$\Lambda(\mathcal{S}, \mathcal{H}) = \Lambda\big(\widetilde{\mathcal{Z}}_{22}^T \widetilde{\mathcal{Z}}_{11}, \widetilde{\mathcal{H}}_{11}\big) = \pm \mathrm{i}\sqrt{\Lambda\big(T_{11}^{-1} H_{11} Z_{11}^{-1} Z_{22}^{-T} H_{22}^T T_{22}^{-T}\big)}. \tag{19}$$

Note that all matrices of the product are upper triangular except H_{22}^T, which is upper quasi-triangular. Hence, the eigenvalue information can be extracted directly from the diagonal 1×1 or 2×2 blocks of the main diagonals. Note that the finite, simple, purely imaginary eigenvalues of the initial matrix pencil correspond to the positive eigenvalues of the generalized matrix product. Hence, these eigenvalues can be computed without any error in their real parts. This leads to a high robustness in algorithms that require these eigenvalues (e. g., in the $\mathcal{H}_\infty$-norm computation [Benner et al. 2012a]). However, if two purely imaginary eigenvalues are very close, they might still be slightly perturbed from an imaginary axis. This essentially depends on the Kronecker structure of a close-by skew-Hamiltonian/Hamiltonian matrix pencil with double purely imaginary eigenvalues. This problem is similar to the Hamiltonian matrix case; see Mehrmann and Xu [2008].

To compute the deflating subspaces we are interested in, it is necessary to compute the structured Schur form of the embedded matrix pencils $\lambda\mathcal{B}_{\mathcal{S}}^r - \mathcal{B}_{\mathcal{H}}^r$. This can be done by computing a finite number of similarity transformations to the subpencil $\lambda\widetilde{\mathcal{Z}}_{22}^T\widetilde{\mathcal{Z}}_{11} - \widetilde{\mathcal{H}}_{11}$ to put $\widetilde{\mathcal{H}}_{11}$ into upper quasi-triangular form. That is, we compute orthogonal matrices $\mathcal{Q}_3$, $\mathcal{Q}_4$, $\mathcal{U}_3$ such that

$$\mathcal{H}_{11} = \mathcal{Q}_3^T \widetilde{\mathcal{H}}_{11} \mathcal{Q}_4, \quad \mathcal{Z}_{11} = \mathcal{U}_3^T \widetilde{\mathcal{Z}}_{11} \mathcal{Q}_4, \quad \mathcal{Z}_{22} = \mathcal{U}_3^T \widetilde{\mathcal{Z}}_{22} \mathcal{Q}_3,$$

where $\mathcal{Z}_{11}$, $\mathcal{Z}_{22}^T$ are upper triangular and $\mathcal{H}_{11}$ is upper quasi-triangular. By setting $\mathcal{Q} = \widetilde{\mathcal{Q}}\left[\begin{smallmatrix} \mathcal{Q}_4 & 0 \\ 0 & \mathcal{Q}_3 \end{smallmatrix}\right]$, $\mathcal{U} = \widetilde{\mathcal{U}}\left[\begin{smallmatrix} \mathcal{U}_3 & 0 \\ 0 & \mathcal{U}_3 \end{smallmatrix}\right]$, $\mathcal{Z}_{12} = \mathcal{U}_3^T \widetilde{\mathcal{Z}}_{12} \mathcal{Q}_3$, and $\mathcal{H}_{12} = \mathcal{Q}_3^T \widetilde{\mathcal{H}}_{12} \mathcal{Q}_3$ we obtain the structured Schur form of $\lambda\mathcal{B}_{\mathcal{S}}^r - \mathcal{B}_{\mathcal{H}}^r$ as $\lambda\widetilde{\mathcal{B}}_{\mathcal{S}}^r - \widetilde{\mathcal{B}}_{\mathcal{H}}^r$ with $\widetilde{\mathcal{B}}_{\mathcal{S}}^r = \mathcal{J}(\widetilde{\mathcal{B}}_{\mathcal{Z}}^r)^T \mathcal{J}^T \widetilde{\mathcal{B}}_{\mathcal{Z}}^r$ and

$$\widetilde{\mathcal{B}}_{\mathcal{Z}}^r := \mathcal{U}^T \mathcal{B}_{\mathcal{Z}}^r \mathcal{Q} = \begin{bmatrix} \mathcal{Z}_{11} & \mathcal{Z}_{12} \\ 0 & \mathcal{Z}_{22} \end{bmatrix},$$

$$\widetilde{\mathcal{B}}_{\mathcal{H}}^r := \mathcal{J}\mathcal{Q}^T \mathcal{J}^T \mathcal{B}_{\mathcal{H}}^r \mathcal{Q} = \begin{bmatrix} \mathcal{H}_{11} & \mathcal{H}_{12} \\ 0 & -\mathcal{H}_{11}^T \end{bmatrix}.$$

Now we can reorder the eigenvalues of $\lambda\widetilde{\mathcal{B}}_{\mathcal{S}}^r - \widetilde{\mathcal{B}}_{\mathcal{H}}^r$ to the top in order to compute the desired deflating subspaces, which is similar to the complex case. Then, for the deflating subspaces, we find a similar result as Theorem 3.2, which we do not state here for brevity.

If the matrix $\mathcal{S}$ is not given in factored form, we need the following slightly modified version of Theorem 3.3 from Benner et al. [2007].

THEOREM 3.4. *Let $\lambda\mathcal{S} - \mathcal{H} \in \mathbb{R}[\lambda]^{2n \times 2n}$ be a skew-Hamiltonian/Hamiltonian matrix pencil. Then there exist orthogonal matrices $\mathcal{Q}_1$, $\mathcal{Q}_2$ such that*

$$\begin{aligned} \mathcal{Q}_1^T \mathcal{S} \mathcal{J} \mathcal{Q}_1 \mathcal{J}^T &= \begin{bmatrix} S_{11} & S_{12} \\ 0 & S_{11}^T \end{bmatrix} && \textit{(skew-Hamiltonian)}, \\ \mathcal{J} \mathcal{Q}_2^T \mathcal{J}^T \mathcal{S} \mathcal{Q}_2 &= \begin{bmatrix} T_{11} & T_{12} \\ 0 & T_{11}^T \end{bmatrix} =: \mathcal{T} && \textit{(skew-Hamiltonian)}, \\ \mathcal{Q}_1^T \mathcal{H} \mathcal{Q}_2 &= \begin{bmatrix} H_{11} & H_{12} \\ 0 & H_{22} \end{bmatrix}, \end{aligned} \tag{20}$$

with the formal matrix product $S_{11}^{-1}H_{11}T_{11}^{-1}H_{22}^T$ *in real periodic Schur form, where* S_{11}, T_{11}, H_{11} *are upper triangular and* H_{22}^T *is upper quasi-triangular.*

PROOF. The proof is done by construction; see Benner et al. [2007]. □

With the notation of Theorem 3.4, we can compute an orthogonal matrix $\widetilde{\mathcal{Q}}$ such that

$$\begin{aligned}
\mathcal{J}\widetilde{\mathcal{Q}}^T\mathcal{J}^T\mathcal{B}^r_{\mathcal{S}}\widetilde{\mathcal{Q}} &= \left[\begin{array}{cc|cc} S_{11} & 0 & S_{12} & 0 \\ 0 & T_{11} & 0 & T_{12} \\ \hline 0 & 0 & S_{11}^T & 0 \\ 0 & 0 & 0 & T_{11}^T \end{array}\right] =: \begin{bmatrix} \widetilde{\mathcal{S}}_{11} & \widetilde{\mathcal{S}}_{12} \\ 0 & \widetilde{\mathcal{S}}_{11}^T \end{bmatrix}, \\
\mathcal{J}\widetilde{\mathcal{Q}}^T\mathcal{J}^T\mathcal{B}^r_{\mathcal{H}}\widetilde{\mathcal{Q}} &= \left[\begin{array}{cc|cc} 0 & H_{11} & 0 & H_{12} \\ -H_{22}^T & 0 & H_{12} & 0 \\ \hline 0 & 0 & 0 & H_{22} \\ 0 & 0 & -H_{11}^T & 0 \end{array}\right] =: \begin{bmatrix} \widetilde{\mathcal{H}}_{11} & \widetilde{\mathcal{H}}_{12} \\ 0 & -\widetilde{\mathcal{H}}_{11}^T \end{bmatrix},
\end{aligned} \tag{21}$$

with $\widetilde{\mathcal{Q}} = \mathcal{P}^T [\begin{smallmatrix} \mathcal{J}\mathcal{Q}_1\mathcal{J}^T & 0 \\ 0 & \mathcal{Q}_2 \end{smallmatrix}]\mathcal{P}$. The spectrum of $\lambda\mathcal{S} - \mathcal{H}$ is given by

$$\Lambda(\mathcal{S}, \mathcal{H}) = \pm \mathrm{i}\sqrt{\Lambda\left(S_{11}^{-1}H_{11}T_{11}^{-1}H_{22}^T\right)}$$

which can be determined by evaluating the entries on the 1×1 and 2×2 diagonal blocks of the matrices only. To put the matrix pencil formed of the matrices in Equation (21) into structured Schur form, we have to triangularize $\lambda\widetilde{\mathcal{S}}_{11} - \widetilde{\mathcal{H}}_{11}$; that is, we determine orthogonal matrices $\mathcal{Q}_3$ and $\mathcal{Q}_4$ such that

$$\mathcal{S}_{11} = \mathcal{Q}_4^T\widetilde{\mathcal{S}}_{11}\mathcal{Q}_3, \quad \mathcal{H}_{11} = \mathcal{Q}_4^T\widetilde{\mathcal{H}}_{11}\mathcal{Q}_3$$

are upper triangular and upper quasi-triangular, respectively. By setting $\mathcal{Q} = \widetilde{\mathcal{Q}}[\begin{smallmatrix} \mathcal{Q}_3 & 0 \\ 0 & \mathcal{Q}_4 \end{smallmatrix}]$, $\mathcal{S}_{12} = \mathcal{Q}_4^T\widetilde{\mathcal{S}}_{12}\mathcal{Q}_4$, and $\mathcal{H}_{12} = \mathcal{Q}_4^T\widetilde{\mathcal{H}}_{12}\mathcal{Q}_4$, we obtain the structured Schur form as

$$\begin{aligned}
\widetilde{\mathcal{B}}^r_{\mathcal{S}} &:= \mathcal{J}\mathcal{Q}^T\mathcal{J}^T\mathcal{B}_{\mathcal{S}}\mathcal{Q} = \begin{bmatrix} \mathcal{S}_{11} & \mathcal{S}_{12} \\ 0 & \mathcal{S}_{11}^T \end{bmatrix}, \\
\widetilde{\mathcal{B}}^r_{\mathcal{H}} &:= \mathcal{J}\mathcal{Q}^T\mathcal{J}^T\mathcal{B}_{\mathcal{H}}\mathcal{Q} = \begin{bmatrix} \mathcal{H}_{11} & \mathcal{H}_{12} \\ 0 & -\mathcal{H}_{11}^T \end{bmatrix}.
\end{aligned}$$

By properly reordering the eigenvalues, we can compute the desired deflating subspaces as explained earlier. A complete algorithm description can be found in Benner et al. [2007]. We omit the details for brevity.

4. IMPLEMENTATION DETAILS

In this section, we focus on implementation details of the algorithms outlined earlier.

4.1. General Remarks

Our subroutines are written by employing the rigorous implementation and documentation standards of the Subroutine Library in Control Theory (SLICOT[1]); see Working Group on Software (WGS) [1996a, 1996b]. The parameters of each SLICOT routine can be classified as follows:

—mode parameters,
—input/output parameters,
—tolerances,

[1] http://slicot.org/.

Hamiltonian	skew-Hamiltonian
$\mathrm{DE} = \begin{bmatrix} e_{11} & d_{11} & d_{12} & d_{13} & \cdots \\ e_{21} & e_{22} & d_{22} & d_{23} & \cdots \\ e_{31} & e_{32} & e_{33} & d_{33} & \cdots \\ \vdots & \vdots & \vdots & \vdots & \ddots \end{bmatrix}$	$\mathrm{DE} = \begin{bmatrix} \star & \star & d_{12} & d_{13} & \cdots \\ e_{21} & \star & \star & d_{23} & \cdots \\ e_{31} & e_{32} & \star & \star & \cdots \\ \vdots & \vdots & \vdots & \vdots & \ddots \end{bmatrix}$

Fig. 1. Storage layout for the (skew-)symmetric submatrices D and E.

—workspace,
—error/warning indicator.

Mode parameters specify the provided functionality with regard to output results and the methods used for the computations. Input/output parameters are usually the dimension of the involved matrices and the matrices themselves with their leading dimensions. The error indicator `INFO` tells the user if an illegal value was used as input (`INFO` returns negative values) or whether an error occurred during program execution (`INFO` returns positive values). A warning indicator `IWARN` informs the user about possibly unreliable or inaccurate results or additional information about the results.

4.2. Storage Layout

Since Hamiltonian and skew-Hamiltonian matrices have certain block structures, we use a packed storage layout proposed in Benner et al. [2000] to avoid saving redundant data. More specifically, if a real $2n \times 2n$ Hamiltonian matrix $\mathcal{H} = \left[\begin{smallmatrix} A & D \\ E & -A^T \end{smallmatrix}\right]$ is given, we save the submatrix A in a conventional $n \times n$ array `A`, the symmetric submatrices D and E are stored in an $n \times (n+1)$ array `DE` such that the upper triangular part of D is stored in `DE(1:n,2:n+1)`, and the lower triangular part of E is stored in `DE(1:n,1:n)`. The skew-symmetric parts of a skew-Hamiltonian matrix are similarly stored with the notable difference that the parts containing the diagonal and the first superdiagonal of the array `DE` are not referenced. See also Figure 1 for an illustration.

Similarly, because every orthogonal or unitary symplectic $2n \times 2n$ matrix has the block structure $\mathcal{U} = \left[\begin{smallmatrix} U_1 & U_2 \\ -U_2 & U_1 \end{smallmatrix}\right]$, we only store the matrix U_1 in an $n \times n$ array `U1` and the matrix U_2 in an $n \times n$ array `U2`.

A similar storage format is also applied to complex skew-Hamiltonian or Hamiltonian matrices. In contrast to the real case, for skew-Hamiltonian matrices, also the parts containing the diagonal and the first superdiagonal of the array `DE` are referenced.

4.3. Panel Blocking for Larger Problems

The problems considered here are usually based on applying sequences of Givens rotations. When updating the involved matrices, we successively have to transform the corresponding rows and columns in each step. However, for larger matrices, this kind of transformations can become very inefficient due to Fortran's memory and cache management. Fortran uses a column-major memory layout; that is, elements of a column are internally stored one after the other. On the other hand, the distance in the internal memory between two successive elements in a row is exactly the leading dimension of that array. Therefore, rows can only be put into the cache memory by caching also the remaining parts of the columns that contain elements of the rows under consideration. For larger arrays, this easily leads to chunk sizes that no longer fit into cache memory.

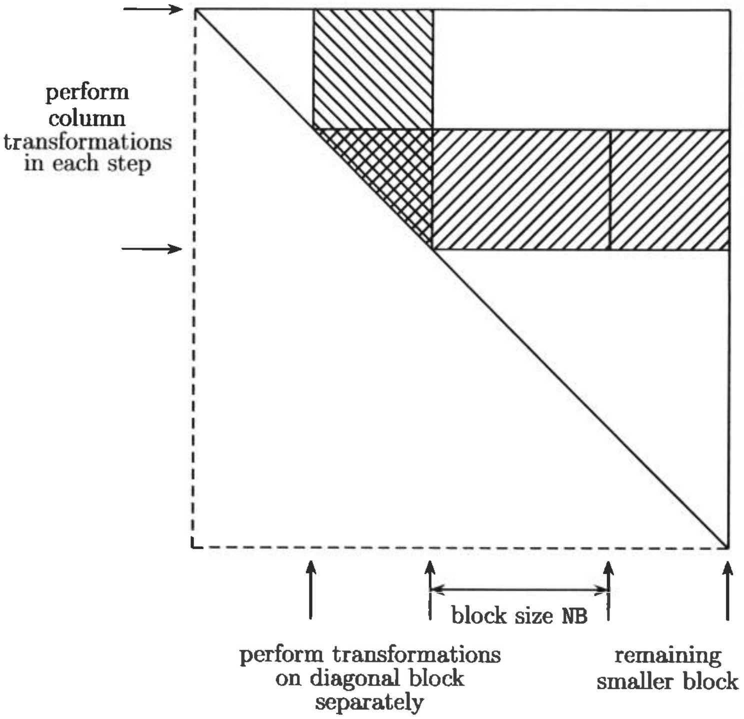
perform column transformations in each step
block size NB
perform transformations on diagonal block separately
remaining smaller block

Fig. 2. Panel blocking technique for an upper triangular matrix.

Therefore, we store the information of a certain number of Givens rotations and apply the row transformations only on panels of block size NB in order to better exploit the data locality.

An example for such a panel update is depicted in Figure 2. It illustrates the blocking technique for an update of a triangular matrix. Updates on columns are always directly applied after the generation of the Givens rotation, whereas rows are split into certain subpanels of maximum block size NB. Note that updates on the diagonal block are done separately because then the remaining parts of the rows have equal size and can therefore be easily decomposed into subblocks. We note that each part of the code has to be blocked in a different way. This is due to different matrix structures or dependencies of the updates and generation of the next Givens rotations. Therefore, sometimes parts of rows have to be updated in each step. We have developed blocked versions for some of our codes, and we will compare them with the unblocked versions in Section 5.

4.4. Overview of the Implemented Fortran Subroutines

Table I contains a brief overview of the main algorithms that have been implemented along with their corresponding Fortran subroutine names. Full details of the individual interfaces and the structure of the call graphs of the driver routines may be found in the user manual that accompanies the software [Benner et al. 2015].

5. NUMERICAL RESULTS

In this section, we present some numerical results of our implementations. The tests have been performed on a 2.6.32-31-generic Ubuntu machine with Intel®Core™2 Quad CPU Q9550 with 2.83GHz in each of the four cores and 8GB RAM. All codes have been compiled using gfortran with the optimization level -O2 (safe optimizations). For

Table I. Overview of the Implemented Fortran Routines

Fortran routine	Algorithm description
ZGHFDF	Computing the eigenvalues and stable deflating subspaces of a complex skew-Hamiltonian/Hamiltonian pencil (factored version)
DGHFST	Computing the eigenvalues of a real skew-Hamiltonian/skew-Hamiltonian pencil (factored version)
ZGHFXC	Moving eigenvalues with negative real parts of a complex skew-Hamiltonian/Hamiltonian pencil in structured Schur form to the leading subpencil (factored version)
ZGHUDF	Computing the eigenvalues and stable deflating subspaces of a complex skew-Hamiltonian/Hamiltonian pencil (unfactored version)
DGHUST	Computing the eigenvalues of a real skew-Hamiltonian/skew-Hamiltonian pencil (unfactored version)
ZGHUXC	Moving eigenvalues with negative real parts of a complex skew-Hamiltonian/Hamiltonian pencil in structured Schur form to the leading subpencil (unfactored version)
DGHFDF	Computing the eigenvalues and stable deflating subspaces of a real skew-Hamiltonian/Hamiltonian pencil (factored version)
DGHURV	Computing the eigenvalues of a real skew-Hamiltonian/Hamiltonian pencil via generalized symplectic URV decomposition (factored version)
DGHFYR	Reducing a special real block (anti-)diagonal skew-Hamiltonian/Hamiltonian pencil in factored form to generalized Schur form (factored version)
DGHFXC	Moving eigenvalues with negative real parts of a real skew-Hamiltonian/Hamiltonian pencil in structured Schur form to the leading subpencil (factored version)
DGHUDF	Computing the eigenvalues and stable deflating subspaces of a real skew-Hamiltonian/Hamiltonian pencil (unfactored version)
DGHUTR	Computing the eigenvalues of a real skew-Hamiltonian/Hamiltonian pencil (unfactored version)
DGHUYR	Reducing a special real block (anti-)diagonal skew-Hamiltonian/Hamiltonian pencil in factored form to generalized Schur form (unfactored version)
DGHUXC	Moving eigenvalues with negative real parts of a real skew-Hamiltonian/Hamiltonian pencil in structured Schur form to the leading subpencil (unfactored version)

better handling of the codes, MEX gateway functions have been written for calling the routines from MATLAB 7.14.0.739 (R2012a). For this purpose, we also use MATLAB's built-in MKL BLAS and LAPACK libraries, which are optimized for using multicore architectures.

5.1. Structure-Preserving Computations

The most important feature of our algorithms is structure-preservation. This means that only reductions that keep the skew-Hamiltonian/Hamiltonian structure are performed. Therefore, only skew-Hamiltonian/Hamiltonian perturbations of the eigenvalues are possible. In particular, simple, finite, purely imaginary eigenvalues stay on the imaginary axis as long as their pairwise distance is sufficiently large. In such a situation, the perturbation off the imaginary axis would not lead to the formation of a quadruple of eigenvalues, which is necessary by the Hamiltonian spectral symmetry.

In Figure 3, some of the computed eigenvalues by the QZ algorithm [Golub and Van Loan 1996] and our new method are depicted. For the tests, we used extended skew-Hamiltonian/Hamiltonian pencils for the $\mathcal{L}_\infty$-norm computation of descriptor systems [Voigt 2010]. The pencils are related to models for constrained mass-spring

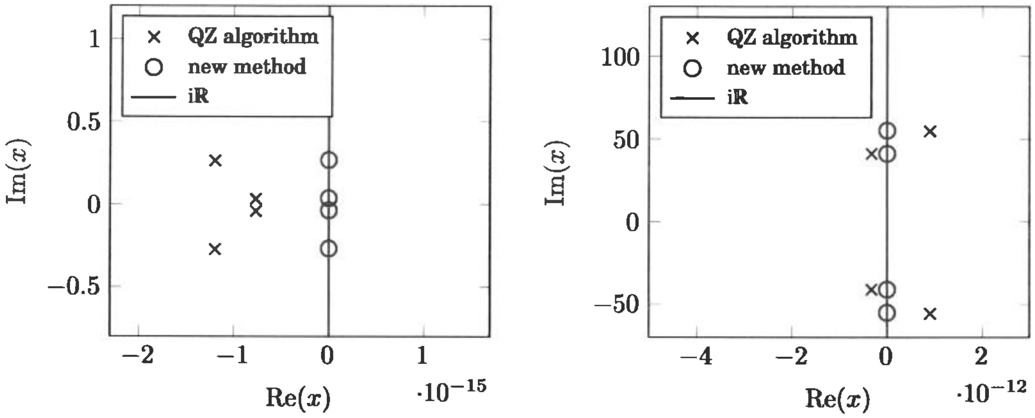

(a) Constrained damped mass-spring system.

(b) Semidiscretized Stokes equation.

Fig. 3. Computed purely imaginary eigenvalues of two skew-Hamiltonian/Hamiltonian example matrix pencils.

systems or semidiscretized Stokes equations (see Mehrmann and Stykel [2005] and references therein). The figure shows that the eigenvalues computed by the standard QZ algorithm are perturbed off the imaginary axis, whereas the new method preserves the eigenvalue symmetry. In particular, the new approach allows a reliable determination of the stable eigenvalues. If we furthermore want to compute the stable deflating subspaces, we have to know the stable eigenvalues in advance. For the first example (Figure 3(a)), the QZ algorithm computes more stable than unstable eigenvalues, which is impossible by theory. Therefore, also the stable deflating subspace computed by this method will have a too large dimension. This undesired behavior is avoided by our method.

A second example that illustrates the superiority of our method arises in the context of gyroscopic systems of the form

$$M\ddot{x}(t) + G\dot{x}(t) + Kx(t) = 0 \tag{22}$$

with $M = M^T > 0$, $G = -G^T$, and $K = K^T$. To analyze stability of such a system, we have to consider the quadratic eigenvalue problem

$$(M\lambda^2 + G\lambda + K)y = 0. \tag{23}$$

It can be shown that a necessary condition for Equation (22) to be stable is that all eigenvalues of Equation (23) are purely imaginary [Lancaster 2013]. A linearization of Equation (23) to second companion form [Tisseur and Meerbergen 2001] leads to an eigenvalue problem for the skew-Hamiltonian/Hamiltonian matrix pencil

$$\lambda \begin{bmatrix} M & G \\ 0 & M \end{bmatrix} - \begin{bmatrix} 0 & -K \\ M & 0 \end{bmatrix}.$$

The example we use here is the "Rolling Tires" system from Benner et al. [2008a] with a system dimension of $n = 2697$. The computed eigenvalues for both the QZ algorithm and our method are depicted in Figure 4. For our algorithm, all eigenvalues are determined to be on the imaginary axis, which means that the necessary stability criterion for the gyroscopic system is fulfilled. However, for the QZ algorithm, this is not the case. Since the QZ algorithm does not respect the skew-Hamiltonion/Hamiltonian structure, all eigenvalues are perturbed off the imaginary axis. Some of them are also very far away from the imaginary axis (the maximum absolute value of the real parts

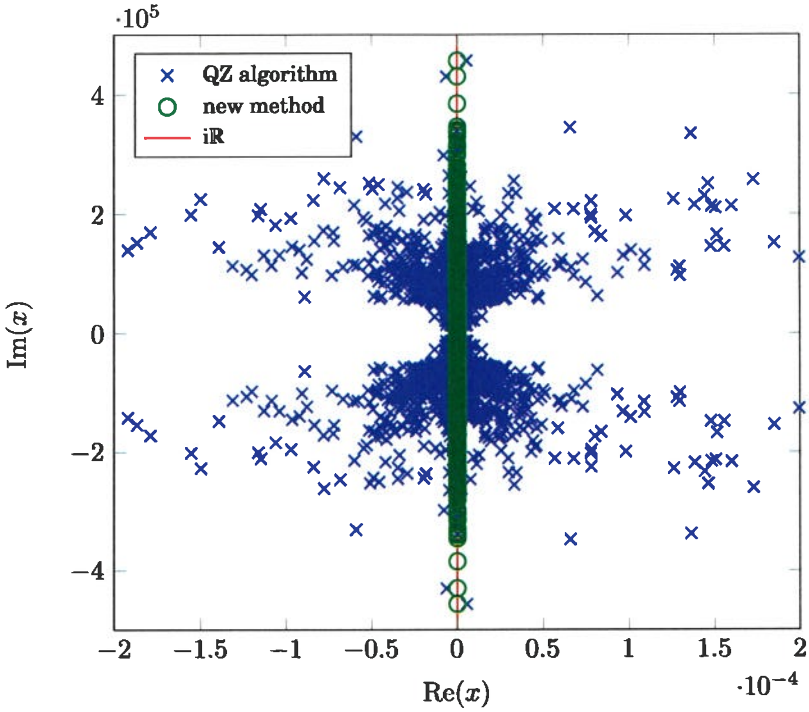

Fig. 4. Computed eigenvalues from a skew-Hamiltonian/Hamiltonian matrix pencil resulting from a linearized gyroscopic system.

is 1.4836e-03). So, in contrast to the structure-preserving approach, one could think that the necessary stability criterion is not fulfilled.

5.2. Solving Algebraic Riccati Equations

In this subsection, we use our algorithms for computing the solution of algebraic Riccati equations and compare these with the results of the MATLAB function `care`. We consider continuous-time Algebraic Riccati Equations (AREs) of the form

$$0 = Q + A^T X + XA - XGX, \tag{24}$$

where $A, G, Q, X \in \mathbb{R}^{n\times n}$. In many problems, the matrices $Q = Q^T$ and $G = G^T$ are given in factored form $Q = C^T \widetilde{Q} C$, $G = BR^{-1}B^T$ with $C \in \mathbb{R}^{p\times n}$, $B \in \mathbb{R}^{n\times m}$, $\widetilde{Q} = \widetilde{Q}^T \in \mathbb{R}^{p\times p}$, and $R = R^T \in \mathbb{R}^{m\times m}$. If $\widetilde{Q} \geq 0$, $R > 0$, (A, B) is stabilizable, and (A, C) is detectable, then Equation (24) has a unique, symmetric positive semidefinite, stabilizing solution X_*.

A popular method for determining X_* is to compute the stable invariant subspace spanned by $\left[\begin{smallmatrix} U_1 \\ U_2 \end{smallmatrix}\right]$ of the Hamiltonian matrix

$$\mathcal{H} = \begin{bmatrix} A & -G \\ -Q & -A^T \end{bmatrix} = \begin{bmatrix} A & -BR^{-1}B^T \\ -C^T\widetilde{Q}C & -A^T \end{bmatrix} \in \mathbb{R}^{2n\times 2n}.$$

If U_1 is invertible, then $X_* = U_2 U_1^{-1}$ (see Abels and Benner [1999] and references therein). Here, we use a slightly more general approach; namely, we compute the right

Table II. Relative Residuals of the Solution of Algebraic Riccati Equations: Comparison of the New Algorithm with Orthogonalization via Pivoted QR Factorization (QRP), Singular Value Decomposition (SVD), and the MATLAB Solver `care`

test #	ex. #	n	m	p	parameters	QRP	SVD	`care`
1	1.1	2	1	2		3.0044e-15	2.5749e-15	3.0062e-15
2	1.2	2	1	2		7.3931e-16	3.4594e-15	6.5338e-16
3	1.3	4	2	4		2.4751e-15	2.4167e-15	3.9430e-15
4	1.4	8	2	8		2.5514e-15	1.5739e-15	1.1924e-15
5	1.5	9	3	9		**8.7957e-15**	2.3342e-13	9.3663e-14
6	1.6	30	3	5		8.8269e-12	4.4861e-12	1.4481e-12
7	2.1	2	1	1	$\varepsilon = 1$	9.0528e-16	9.5989e-16	7.5037e-16
8	2.1	2	1	1	$\varepsilon = 10^{-6}$	1.7361e-10	3.2218e-10	**0**
9	2.2	2	2	1	$\varepsilon = 1$	5.5948e-16	3.7261e-16	1.1068e-15
10	2.2	2	2	1	$\varepsilon = 10^{-8}$	1.5895e-09	7.7370e-10	2.3218e-09
11	2.3	2	1	2	$\varepsilon = 1$	7.3951e-16	1.4259e-15	1.1378e-15
12	2.3	2	1	2	$\varepsilon = 10^{6}$	2.0448e-10	3.7537e-11	**6.5854e-13**
13	2.3	2	1	2	$\varepsilon = 10^{-6}$	**1.6745e-21**	4.6784e-18	6.8373e-20
14	2.4	2	2	2	$\varepsilon = 1$	**0**	1.2684e-14	1.1531e-15
15	2.4	2	2	2	$\varepsilon = 10^{-7}$	2.9441e-15	1.1608e-14	**1.6454e-16**
16	2.5	2	1	2	$\varepsilon = 1$	1.4121e-15	1.3570e-15	1.9343e-15
17	2.5	2	1	2	$\varepsilon = 0$	3.6694e-05	1.2326e-06	**1.2232e-15**
18	2.6	3	3	3	$\varepsilon = 1$	5.8902e-15	3.8570e-15	5.7262e-15
19	2.6	3	3	3	$\varepsilon = 10^{6}$	4.7596e+02	4.4341e+02	6.3670e+02
20	2.7	4	1	2	$\varepsilon = 1$	2.4085e-16	1.6736e-16	1.4054e-15
21	2.7	4	1	2	$\varepsilon = 10^{-6}$	1.9697e-08	3.2989e-11	1.3429e-11
22	2.8	4	1	1	$\varepsilon = 1$	7.4186e-16	4.0395e-15	5.6954e-15
23	2.8	4	1	1	$\varepsilon = 10^{-6}$	3.8032e-15	1.0134e-15	4.6214e-15
24	2.9	55	2	10	#1	1.0737e-11	5.7755e-12	**2.4757e-13**
25	3.1	9	5	4		3.8305e-15	2.6481e-15	3.2909e-15
26	3.1	39	20	19		3.4076e-15	4.6692e-15	8.0452e-15
27	3.2	8	8	8		2.9567e-15	2.2579e-15	3.7270e-15
28	3.2	64	64	64		9.8352e-15	8.8604e-15	1.2277e-14
29	4.1	21	1	1	$q = r = 1.0$	1.0359e-06	4.4380e-07	6.8088e-07
30	4.1	21	1	1	$q = r = 100.0$	2.1010e-05	2.1627e-05	6.3995e-05
31	4.2	20	1	1	$a = 0.05,\ b = c = 0.1,$ $[\beta_1, \beta_2] = [0.1, 0.5],$ $[\gamma_1, \gamma_2] = [0.1, 0.5]$	**1.4274e-17**	1.1291e-13	1.8773e-13
32	4.2	100	1	1	$a = 0.01,\ b = c = 1.0,$ $[\beta_1, \beta_2] = [0.2, 0.3],$ $[\gamma_1, \gamma_2] = [0.2, 0.3]$	**1.3742e-15**	1.2528e-12	3.5524e-12
33	4.3	60	2	60	$\ell = 30,\ \mu = 4.0,$ $\delta = 4.0,\ \kappa = 1.0$	7.8279e-15	7.9629e-15	2.6545e-14
34	4.4	421	211	211		5.1450e-03	1.0845e-05	**7.9411e-07**

stable deflating subspace of the skew-Hamiltonian/Hamiltonian matrix pencil

$$\lambda\mathcal{S} - \mathcal{H} = \lambda\begin{bmatrix} I_n & 0 \\ 0 & I_n \end{bmatrix} - \begin{bmatrix} A & -G \\ -Q & -A^T \end{bmatrix} \in \mathbb{R}[\lambda]^{2n\times 2n}$$

which is equal to the stable invariant subspace of $\mathcal{H}$.

For benchmarking, we use the examples collected in Abels and Benner [1999], which are often difficult to solve due to ill-conditioning of the ARE or the existence of eigenvalues of $\mathcal{H}$ close to the imaginary axis. In Table II, the relative residuals for each

Table III. Comparison of Runtimes for the Real Case (Measured in Secs.)

	Eigenvalues Only		Eigenvalues and Deflating Subspaces	
Problem Size	DGGEV	DGHUTR	DGGES	DGHUDF
2	3.2480e-06	2.2000e-06	7.7860e-06	2.1138e-05
4	1.1510e-05	1.3725e-05	4.3221e-05	1.1633e-04
8	3.7886e-05	7.3677e-05	1.4393e-04	3.6971e-04
16	1.2640e-04	1.9300e-04	3.6360e-04	1.3859e-03
32	7.1310e-04	7.3620e-04	1.7058e-03	5.0400e-03
64	3.0412e-03	3.0708e-03	8.3355e-03	2.5425e-02
128	1.8980e-02	1.6620e-02	4.3790e-02	1.1256e-01
256	1.4190e-01	1.0272e-01	2.8654e-01	5.8121e-01
512	1.4790e+00	8.9793e-01	2.5960e+00	3.9449e+00
1024	2.2127e+01	1.2964e+01	4.8888e+01	4.5998e+01
2048	4.2508e+02	2.6144e+02	5.6186e+02	6.3338e+02
4096	2.9650e+03	2.8367e+03	4.2058e+03	5.5788e+03

individual problem are presented. We compare the skew-Hamiltonian/Hamiltonian pencil approach with orthogonalization via pivoted QR factorization (QRP), Singular Value Decomposition (SVD), and the MATLAB solver (care). To ensure comparability, we use the same scaling technique for the ARE for both our codes and care (by calling arescale in MATLAB). Except for one example (which care also could not solve), our codes could compute X_* in all tests. The relative residuals are most often of the same order of magnitude. For five problems, our codes obtained better results for at least one orthogonalization option (for tests 5, 13, 14, 31, 32, the relative residual is at least one order of magnitude smaller than the one of care). On the other hand, care performed better for six examples (8, 12, 15, 17, 24, 34). In particular, for example 17, the difference is about 10 orders of magnitude; for the other examples (except for example 8) the difference is about one order of magnitude. Note that example 17 is difficult to solve in the sense that the pencil $\lambda\mathcal{S} - \mathcal{H}$ has eigenvalues on the imaginary axis; that is, even though the ARE is solvable, it is on the boundary of unsolvability. To construct the stabilizing solution of the ARE via deflating subspaces, one has to include a certain subspace of $\mathrm{Defl}_0(\mathcal{S}, \mathcal{H})$ which is, however, neither correctly extracted by a pivoted QR decomposition nor an SVD. On the other hand, by determining the desired deflating subspace by a non-pivoted QR decomposition, we obtain a relative residual of 1.2232e-15. This indicates that, for this orthogonalizaton scheme, the correct subspace was extracted. This behavior does not, however, turn over to many of the other examples.

A similar overall picture is achieved when looking at the relative errors compared to the analytic solution if it is known. We omit this analysis since it does not give significantly more information. In conclusion, both approaches give results of similar quality, even though our codes are not specifically designed for solving AREs.

5.3. Comparison of Runtimes

In this subsection, we discuss the runtimes of our codes and compare them with standard implementations included in LAPACK. The results are listed in Tables III and IV, respectively. In Figure 5, the runtime ratios of the new codes compared to MATLAB's LAPACK implementations are depicted to summarize these results. In general, pure eigenvalue computations are much faster than the computation of both eigenvalues and deflating subspaces. The reason is that for the subspace computation, the transformation matrices for the embedded pencils (*of double size*) are accumulated in the final step. However, during our tests, we often observe that LAPACK routines, even though they are faster, are not able to solve some (random) examples. Especially for

Table IV. Comparison of Runtimes for the Complex Case (Measured In Secs.)

	Eigenvalues Only		Eigenvalues and Deflating Subspaces	
Problem Size	ZGGEV	DGHUST	ZGGES	ZGHUDF
2	7.7400e-06	4.7300e-06	2.7047e-05	4.1847e-05
4	2.3252e-05	2.2831e-05	5.2271e-05	9.3827e-05
8	8.2346e-05	7.5673e-05	1.2291e-04	2.2438e-04
16	3.1020e-04	3.1190e-04	4.6900e-04	7.7210e-04
32	1.4953e-03	1.4844e-03	2.5219e-03	3.4171e-03
64	8.7930e-03	9.0812e-03	1.4392e-02	1.9041e-02
128	5.8440e-02	5.6700e-02	9.2550e-02	1.1988e-01
256	4.5301e-01	4.5600e-01	6.2856e-01	9.6518e-01
512	3.4875e+00	7.6826e+00	4.6978e+00	1.4286e+01
1024	3.8185e+01	1.4554e+02	5.6904e+01	2.6081e+02
2048	4.9624e+02	1.2935e+03	8.2872e+02	2.1489e+03
4096	4.8410e+03	1.0849e+04	7.7507e+03	1.7189e+04

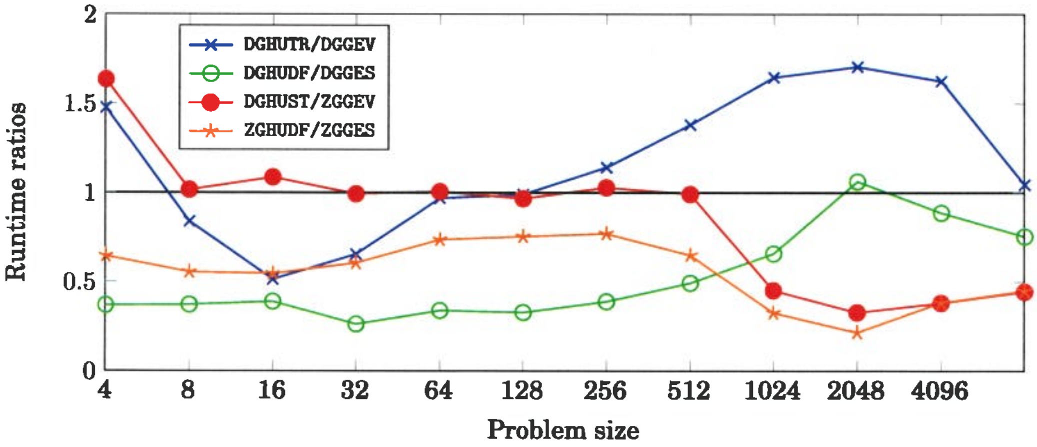

Fig. 5. Runtime ratios of the new routines compared to LAPACK software.

larger problems, INFO = N+2 is returned, which indicates that the desired reordering of the eigenvalues could not be successfully performed. On the other hand, our solvers could always return meaningful results. Note that LAPACK routines can much better exploit blocked codes of Level 3 BLAS, which is not the case for our codes since they are algorithmically based on Givens rotations. Even though the panel blocking technique we present here gives some improvements for larger examples, there is still the question of whether one can find better ways of blocking our codes.

There are also significant differences in the behavior of the real and complex codes. The real codes have relatively constant runtime ratios for small and medium-size problems up to orders of about 128. Then, they increase up to order 2,048 and then decrease again. However, for the complex codes, the runtime ratios are constant for problems up to order 256 and get significantly slower for larger problems. The main reason for this qualitatively different behavior is that the complex codes need significantly more memory and also more transfers between the different levels of the memory hierarchy. Fortunately, for larger problems, we have developed blocked codes that are able to avoid this slowdown (see also Subsection 5.5).

Table V. Comparison of the Errors of the Eigenvalues

	Real Case		Complex Case	
	unfactored	factored	unfactored	factored
$10^{-17} \leq \kappa_{\max} < 10^{-16}$	0	0	29	44
$10^{-18} \leq \kappa_{\max} < 10^{-17}$	825	805	932	926
$10^{-19} \leq \kappa_{\max} < 10^{-18}$	155	162	39	30
$10^{-20} \leq \kappa_{\max} < 10^{-19}$	6	17	0	0
$\kappa_{\max} < 10^{-20}$	14	16	0	0

Table VI. Comparison of the Errors of the Deflating Subspaces

	Real Case		Complex Case	
	unfactored	factored	unfactored	factored
$10^{-11} \leq \alpha < 10^{-10}$	1	0	0	0
$10^{-12} \leq \alpha < 10^{-11}$	9	11	0	3
$10^{-13} \leq \alpha < 10^{-12}$	82	96	38	62
$10^{-14} \leq \alpha < 10^{-13}$	900	888	962	935
$10^{-15} \leq \alpha < 10^{-14}$	8	5	0	0

5.4. Factored Versus Unfactored Matrix Pencils

In this subsection, we compare the results of the previous subsection with the factored versions of the algorithms with respect to accuracy, memory requirements, and speed.

5.4.1. Accuracy. We begin with an analysis of the obtained accuracy. We performed tests on random skew-Hamiltonian/Hamiltonian pencils of order 40. For the factored algorithms, we choose $\mathcal{Z} = [\begin{smallmatrix} A & 0 \\ 0 & I_{20} \end{smallmatrix}]$ with a random matrix A. Then we can easily form

$$\mathcal{S} = \mathcal{J}\mathcal{Z}^H\mathcal{J}^T\mathcal{Z} = \begin{bmatrix} A & 0 \\ 0 & A^H \end{bmatrix}$$

without any rounding error. This allows a fair comparison between the codes for factored and unfactored problems. First, we analyze the accuracy of the computed eigenvalues. Therefore, we perform 1,000 random tests and compute the maximum of the reciprocal condition numbers $\kappa_{\max}$ of the matrices $\lambda_j\mathcal{S} - \mathcal{H}$, $j = 1, \ldots, 20$ for each problem. The reciprocal condition numbers define the closeness to singularity and should be zero in theory. Thus, small values $\kappa_{\max}$ indicate a high accuracy. We divide the computed results into different classes and list the number of elements in each class in Table V. Furthermore, we observe that, in the real case, the unfactored codes were more accurate for 500 examples. For the complex case, this was the case for 516 examples. We can conclude that the computed eigenvalues are similarly accurate for both types of codes.

We also have a look at the accuracy of the deflating subspaces. Again, we perform 1,000 random tests. With the computed stable deflating subspace $\operatorname{im}\mathcal{Q}$, we measure the error by determining the angle α between the subspaces $\operatorname{im}\mathcal{S}\mathcal{Q}$ and $\operatorname{im}\mathcal{H}\mathcal{Q}$. In our tests, $\mathcal{S}$ and $\mathcal{H}$ are nonsingular and thus, by the definition of a deflating subspace, $\operatorname{im}\mathcal{S}\mathcal{Q} = \operatorname{im}\mathcal{H}\mathcal{Q}$ is satisfied in theory (i.e., $\alpha = 0$). We divide the results into classes, which are listed in Table VI. Now, the unfactored version is more accurate for 615 examples in the real case and for 592 examples in the complex case, respectively. Therefore, we can conclude that the subspace computation is slightly more accurate in the unfactored case.

5.4.2. Speed and Memory Requirements. We briefly compare the timing results of the factored and unfactored codes that are listed in Table VII. A run of the factored versions

Table VII. Comparison of Runtimes for Factored and Unfactored Versions (Measured in Secs.)

	Real Case		Complex Case	
Problem Size	unfactored	factored	unfactored	factored
2	2.1149e-05	3.7359e-05	4.1219e-05	7.4963e-05
4	5.3765e-05	9.4412e-05	8.9305e-05	1.8112e-04
8	3.6373e-04	5.1282e-04	2.3065e-04	4.2514e-04
16	1.4868e-03	1.8846e-03	7.5680e-04	1.1702e-03
32	5.9223e-03	7.8657e-03	3.2732e-03	5.6365e-03
64	2.3258e-02	3.1986e-02	1.8261e-02	2.8526e-02
128	1.0901e-01	1.4402e-01	1.1473e-01	1.9216e-01
256	5.7424e-01	7.9756e-01	9.2289e-01	1.6150e+00
512	3.8463e+00	6.1073e+00	1.4380e+01	3.3246e+01
1024	4.6299e+01	1.0119e+02	2.5326e+02	4.1394e+02
2048	6.0400e+02	9.5667e+02	2.0491e+03	3.5848e+03
4096	5.4444e+03	7.9957e+03	1.6688e+04	2.8164e+04

needs approximately 1.5–2 times as long as one of the unfactored versions. This is simply due to the fact that also more matrix entries (usually ≈50% more) have to be updated within the factored codes. Also, this higher amount of matrices has to be stored, which leads to an approximately 50% higher memory usage.

5.4.3. Conclusion. In conclusion, we can say that one should always use the unfactored version of the code whenever the matrix $\mathcal{S}$ is explicitly given or can be formed without any rounding errors. This is due to the lower accuracy, larger runtimes, and higher memory usage of the factored versions. However, one might think of situations where only the factor $\mathcal{Z}$ is known and it is not possible to appropriately form $\mathcal{S}$ due to numerical errors. Then we still recommend using the factored versions even in the presence of the disadvantages just mentioned.

5.5. Blocked Versus Unblocked Code

As already mentioned, the routines get relatively slow if the problem gets too large. This is due to unoptimized cache usage. Therefore, we have implemented the unfactorized algorithms using the panel blocking technique from Subsection 4.3. For illustration, we generated a random example of order 2,048 and compared the runtimes of the unblocked code with those of the blocked code for different block sizes `NB`. The results can be found in Table VIII. The smallest runtimes are marked in boldface font. The time savings can be significant. For computing the eigenvalues of a complex pencil, the reduction in runtime can be up to 50% compared to the unblocked code. Note that there is only a slight speedup for the subspace computation in the real case since the time-consuming routine `DGHUYR` cannot be blocked. Mostly, the best timings are attained for `NB` = 8; however, similar results are observed for all `NB` = 4, . . . , 128, so the choice of `NB` is flexible. An important point is that the problem must be sufficiently large in order to benefit from the panel blocking; otherwise, one would even lose performance, especially for small block sizes.

Finally, we also compare the performance of our blocked codes for `NB` = 8 with LAPACK for problem sizes of 512 to 4,096. We refer to Figure 6 for the specific LAPACK routines we used for our comparison and the corresponding runtime ratios. For real problems, we can achieve good speedups compared to LAPACK. When computing only the eigenvalues, we can achieve a speedup factor of about 3.5. When we also compute the deflating subspaces, we still get a factor of 1.2, so we are still faster than LAPACK. However, this is no longer the case when we consider complex problems. In this case,

Table VIII. Comparison of Runtimes for Blocked and Unblocked Code (Measured in Secs.)

	Eigenvalues Only		Eigenvalues and Deflating Subspaces	
Block Size NB	real case	complex case	real case	complex case
unblocked	224.23	1332.72	582.65	2173.03
1	200.91	922.11	546.95	1644.15
2	147.87	738.48	517.41	1458.51
4	133.90	662.78	483.16	1365.91
8	**132.31**	**657.39**	466.02	**1345.67**
16	146.86	680.06	470.36	1383.82
32	139.47	680.46	469.58	1363.19
64	138.72	672.18	469.72	1376.00
128	139.44	700.46	**459.48**	1400.46
256	139.62	1024.32	468.70	1775.13
512	151.18	1116.98	482.61	1844.09
1024	216.94	1165.43	548.82	1955.30
2048	210.05	1244.88	555.28	2025.61

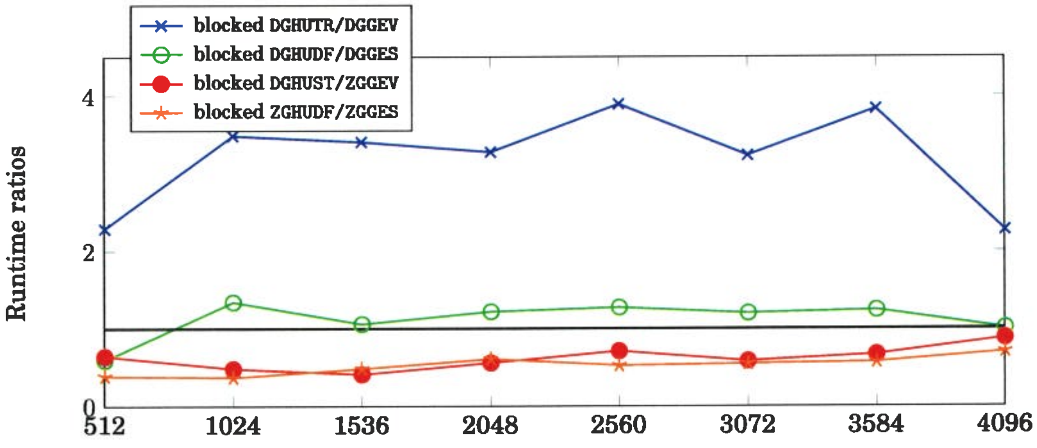

Fig. 6. Runtime ratios of the blocked codes compared to LAPACK software for larger problem sizes.

we achieve a slowdown by a factor between 0.4 to 0.9, but the blocked codes are still faster than the unblocked ones.

6. SUMMARY

We presented algorithms that can be used to compute the eigenvalues and deflating subspaces of skew-Hamiltonian/Hamiltonian matrix pencils in a structure-preserving way, which may lead to higher accuracy, reliability, and computational performance. Applications based on matrix pencils of this structure have been introduced to show the importance of our considerations. Moreover, we presented details of the implementation of the algorithms in Fortran 77. Numerical examples have demonstrated the increased reliability since critical purely imaginary eigenvalues are not perturbed off the imaginary axis (as long as their pairwise distance is large enough). This has also allowed the safe computation of the associated stable deflating subspaces of the pencil since the perturbation of eigenvalues from the left into the right half-plane (or vice versa) is avoided. On the other hand, the runtimes are often higher compared to LAPACK routines. However, a panel blocking technique has significantly improved performance for larger problems.

REFERENCES

J. Abels and P. Benner. 1999. *CAREX - A Collection of Benchmark Examples for Continuous-Time Algebraic Riccati Equations (Version 2.0)*. SLICOT Working Note 1999-14. Niconet e. V.

A. C. Antoulas. 2005. *Approximation of Large-Scale Dynamical Systems*. SIAM, Philadelphia, PA.

P. Benner, R. Byers, and E. Barth. 2000. Algorithm 800: Fortran 77 subroutines for computing the eigenvalues of Hamiltonian matrices I: The square-reduced method. *ACM Transactions on Mathematical Software* 26, 1 (2000), 49–77. DOI: http://dx.doi.org/10.1145/347837.347852

P. Benner, R. Byers, P. Losse, V. Mehrmann, and H. Xu. 2007. Numerical solution of real skew-Hamiltonian/Hamiltonian eigenproblems. (Nov. 2007). Unpublished report.

P. Benner, R. Byers, V. Mehrmann, and H. Xu. 2002. Numerical computation of deflating subspaces of skew-Hamiltonian/Hamiltonian pencils. *SIAM Journal of Matrix Analysis Applications* 24, 1 (2002), 165–190.

P. Benner, H. Fassbender, and M. Stoll. 2008a. Solving large-scale quadratic eigenvalue problems with Hamiltonian eigenstructure using a structure-preserving Krylov subspace method. *Electronic Transactions on Numerical Analysis* 29 (2008), 212–229.

P. Benner, P. Losse, V. Mehrmann, L. Poppe, and T. Reis. 2008b. γ-iteration for descriptor systems using structured matrix pencils. In *Proceedings of the International Symposium on Mathematical Theory of Networks and Systems*. Blacksburg VA.

P. Benner, V. Sima, and M. Voigt. 2012a. $\mathcal{L}_\infty$-norm computation for continuous-time descriptor systems using structured matrix pencils. *IEEE Transactions on Automated Control* 57, 1 (2012), 233–238. DOI: http://dx.doi.org/10.1109/TAC.2011.2161833

P. Benner, V. Sima, and M. Voigt. 2012b. Robust and efficient algorithms for $\mathcal{L}_\infty$-norm omputations for descriptor systems. In *Proceedings of the 7th IFAC Symposium on Robust Control Design*. Aalborg, Denmark, 195–200. DOI: http://dx.doi.org/10.3182/20120620-3-DK-2025.00114

P. Benner, V. Sima, and M. Voigt. 2015. *SHHEIG Users' Guide*.

A. Bojanczyk, G. H. Golub, and P. Van Dooren. 1992. The periodic Schur decomposition. Algorithms and applications. In *Advanced Signal Processing Algorithms, Architectures, and Implementations III (Proc. SPIE)*, F. T. Luk (Ed.), Vol. 1770. 31–42.

T. Brüll and V. Mehrmann. 2007. *STCSSP: A FORTRAN 77 Routine to Compute a Structured Staircase Form for a (Skew-)SymMetRic / (Skew-)SymMetRic Matrix Pencil*. Preprint 31-2007. Institut für Mathematik, TU Berlin.

R. Byers, V. Mehrmann, and H. Xu. 2007. A structured staircase algorithm for skew-symmetric/symmetric pencils. *Electronic Transactions on Numerical Analysis* 26 (2007), 1–33.

L. Dai. 1989. *Singular Control Systems*. Lecture Notes in Control and Inform. Sci., Vol. 118. Springer-Verlag, Heidelberg.

G. H. Golub and C. F. Van Loan. 1996. *Matrix Computations* (third ed.). The John Hopkins University Press, Baltimore/London.

J. J. Hench and A. J. Laub. 1994. Numerical solution of the discrete-time periodic Riccati equation. *IEEE Transactions on Automatic Control* 39, 6 (1994), 1197–1210.

A. Kawamoto, K. Takaba, and T. Katayama. 1999. On the generalized algebraic Riccati equation for continuous-time descriptor systems. *Linear Algebra and Its Applications* 296 (1999), 1–14.

P. Lancaster. 2013. Stability of linear gyroscopic systems: A review. *Linear Algebra and Its Applications* 439, 3 (2013), 686–706. Special Issue in Honor of Harm Bart.

P. Losse. 2012. *The $\mathcal{H}_\infty$ Optimal Control Problem for Descriptor Systems*. Dissertation. Fakultät für Mathematik, Technische Universität Chemnitz.

P. Losse, V. Mehrmann, L. Poppe, and T. Reis. 2008. The modified optimal $\mathcal{H}_\infty$ control problem for descriptor systems. *SIAM Journal of Control Optimization* 47, 6 (2008), 2795–2811.

C. Mehl. 1999. *Compatible Lie and Jordan Algebras and Applications to Structured Matrices and Pencils*. Dissertation. Chemnitz University of Technology, Faculty of Mathematics, Germany, Berlin.

C. Mehl. 2000. Condensed forms for skew-Hamiltonian/Hamiltonian pencils. *SIAM Journal on Matrix Anaysis and Applications* 21, 2 (2000), 454–476. DOI: http://dx.doi.org/10.1137/S0895479898336513

V. Mehrmann. 1991. *The Autonomous Linear Quadratic Control Problem, Theory and Numerical Solution*. Lecture Notes in Control and Inform. Sci., Vol. 163. Springer-Verlag, Heidelberg.

V. Mehrmann and T. Stykel. 2005. Balanced truncation model reduction for large-scale systems in descriptor form. In *Dimension Reduction of Large-Scale Systems*, P. Benner, V. Mehrmann, and D. Sorensen (Eds.). Lect. Notes Comput. Sci. Eng., Vol. 45. Springer-Verlag, Berlin, Chapter 3, 89–116.

V. Mehrmann and H. Xu. 2008. Perturbation of purely imaginary eigenvalues of Hamiltonian matrices under structured perturbations. *Electronic Journal of Linear Algebra* 17 (2008), 234–257.

Working Group on Software (WGS). 1996a. *SLICOT Contributors' Kit 2.1*. Eindhoven University of Technology, Eindhoven, The Netherlands. WGS Report 96-2.

Working Group on Software (WGS). 1996b. *SLICOT Implementation and Documentation Standards*. Eindhoven University of Technology, Eindhoven, The Netherlands. WGS Report 96-1.

L. S. Pontryagin, V. Boltyanskii, R. Gamkrelidze, and E. Mishenko. 1962. *The Mathematical Theory of Optimal Processes*. Interscience, New York.

L. Poppe, C. Schröder, and I. Thies. 2009. *PEPACK: A Software Package for Computing the Numerical Solution of Palindromic and Even Eigenvalue Problems using the Pencil Laub Trick*. Preprint 22-2009. Institut für Mathematik, Technische Universität Berlin.

T. Reis. 2011. Lur'e equations and even matrix pencils. *Linear Algebra and Its Applications* 434, 1 (2011), 152–173.

T. Reis, O. Rendel, and M. Voigt. 2015. The Kalman-Yakubovich-Popov inequality for differential-algebraic systems. *Linear Algebra and Its Applications* 485 (2015), 153–193.

F. Tisseur and K. Meerbergen. 2001. The qadratic eigenvalue problem. *SIAM Review* 43, 2 (2001), 235–286.

M. Voigt. 2010. *$\mathcal{L}_\infty$-Norm Computation for Descriptor Systems*. Diploma Thesis. Chemnitz University of Technology, Faculty of Mathematics, Germany.

M. Voigt. 2015. *On Linear-Quadratic Optimal Control and Robustness of Differential-Algebraic Systems*. Dissertation. Fakultät für Mathematik, Otto-von-Guericke-Universität Magdeburg. Accepted.

K. Zhou and J. D. Doyle. 1998. *Essentials of Robust Control* (1st ed.). Prentice Hall, Upper Saddle River, NJ.

Received July 2013; revised July 2015; accepted August 2015